Development/Plasticity/Repair

A New Prospero and *microRNA-279* Pathway Restricts CO_2 Receptor Neuron Formation

Marion Hartl, Laura F. Loschek, Daniel Stephan, K. P. Siju, Christiane Knappmeyer, and Ilona C. Grunwald Kadow
Max-Planck Institute of Neurobiology, Sensory Neurogenetics Research Group, 82152 Martinsried, Germany

CO_2 sensation represents an interesting example of nervous system and behavioral evolutionary divergence. The underlying molecular mechanisms, however, are not understood. Loss of *microRNA-279* in *Drosophila melanogaster* leads to the formation of a CO_2 sensory system partly similar to the one of mosquitoes. Here, we show that a novel allele of the pleiotropic transcription factor Prospero resembles the *miR-279* phenotype. We use a combination of genetics and *in vitro* and *in vivo* analysis to demonstrate that Pros participates in the regulation of *miR-279* expression, and that reexpression of *miR-279* rescues the *pros* CO_2 neuron phenotype. We identify common target molecules of *miR-279* and Pros in bioinformatics analysis, and show that overexpression of the transcription factors Nerfin-1 and Escargot (Esg) is sufficient to induce formation of CO_2 neurons on maxillary palps. Our results suggest that Prospero restricts CO_2 neuron formation indirectly via *miR-279* and directly by repressing the shared target molecules, Nerfin-1 and Esg, during olfactory system development. Given the important role of Pros in differentiation of the nervous system, we anticipate that miR-mediated signal tuning represents a powerful method for olfactory sensory system diversification during evolution.

Introduction

Sensory systems of animals match distinct ecological niches. Insects use olfactory cues to navigate to food sources and oviposition sites, and to avoid danger. Hence, olfactory organs are highly specialized, and specific environmental cues elicit highly species-specific behaviors. One example is CO_2. While attractive to mosquitoes, fruit flies show a robust avoidance behavior to even low levels of CO_2 (Gibson, 1996; Suh et al., 2004).

In both fruit flies and mosquitoes, specialized sensory structures on the third segment of the antenna or on the maxillary palp (MP) contain olfactory receptor neurons (ORN) that express receptors tuned to specific odors (Vosshall and Stocker, 2007). In *Drosophila*, two receptors expressed in the same ORN on the antenna, Gr21a and Gr63a, are necessary and sufficient to detect CO_2 and to elicit CO_2-mediated escape responses (Jones et al., 2007; Kwon et al., 2007). In contrast to *Drosophila*, mosquitoes carry CO_2 receptor neurons on their MP (Grant et al., 1995; Jones et al., 2007; Lu et al., 2007). In addition to this peripheral difference, CO_2 ORN axons innervate different glomeruli in the antennal lobe (AL) in the brain. *Drosophila* Gr21a/Gr63a-expressing neurons on the antenna innervate a ventral glomerulus, whereas mosquito CO_2 ORNs target medial glomeruli, which in both of these species respond to food odors (Suh et al., 2004; Vosshall and Stocker, 2007). Possibly, these peripheral and central changes contributed to the behavioral divergence of mosquito and fruit fly (Cayirlioglu et al., 2008; Jones, 2008; Ramdya and Benton, 2010).

We have recently reported that loss of *microRNA-279* leads to formation of ectopic CO_2 neurons on MPs of fruit flies, suggesting a potential involvement of *miR-279* in CO_2 sensory system divergence (Cayirlioglu et al., 2008).

Here, we addressed the mechanistic role of *miR-279* in the development of MP CO_2 neurons. We show that mutations of the atypical homeobox transcription factor Prospero result in a *miR-279* phenotype. Consistent with Prospero's previously reported role in sensory bristles and antenna (Manning and Doe, 1999; Reddy and Rodrigues, 1999; Sen et al., 2003), we find that Pros distinguishes the neuronal pIIb lineage also in MP olfactory sensilla. A new hypomorphic allele of *pros* revealed that in addition, Pros restricts the number of neurons in specific olfactory sensilla. In mutant MPs, CO_2 ORNs are formed as an extra neuron within certain MP sensilla. We apply genetic analysis and *in vitro* assays to show that Pros is involved in the transcriptional regulation of *miR-279*, and that reexpression of *miR-279* in *pros* mutants rescues the *pros* CO_2 neuron phenotype. Using RNAi, loss of function analysis, and overexpression, we demonstrate that upregulation of two Pros and *miR-279* target genes, *nerfin-1* and *escargot*, is necessary and sufficient for the formation and mistargeting of MP CO_2 neurons. Together, our data suggest that Pros regulates *miR-279* expression to enhance its own repressor activ-

Received May 25, 2011; revised Sept. 7, 2011; accepted Sept. 11, 2011.

Author contributions: M.H., L.F.L., and I.C.G.K. designed research; M.H., L.F.L., D.S., K.P.S., C.K., and I.C.G.K. performed research; M.H., L.F.L., D.S., K.P.S., and I.C.G.K. analyzed data; M.H., L.F.L., and I.C.G.K. wrote the paper.

This work was supported by an Emmy-Noether grant of the German Research Foundation and the career development Award of the Human Frontiers Science Organization to I.G.K. The Max Planck Society provided further support through funds to I.G.K. We are very grateful to L. Zipursky and P. Cayirlioglu Volkan for discussions and sharing data in the earlier stages of this work. We thank J. F. Ferveur, A. Brand, C. Doe, T. Cook, S. Cohen, T. Suzuki, and F. Matsuzuki for providing important reagents and fly stocks. We acknowledge the Bloomington, Kyoto, and VDRC stock centers for providing fly stocks. We thank R. Klein, T. Suzuki, F. Schnorrer, and members of the laboratories for helpful discussions and comments on this manuscript.

The *pros*^{IG2227} mutant was discovered as part of a screen that was performed by I.C.G.K. and P. Cayirlioglu Volkan while they were postdoctoral fellows in the Zipursky lab.

The authors declare no financial conflicts interest.

Correspondence should be addressed to Ilona C. Grunwald Kadow, Sensory Neurogenetics Research Group, Max-Planck Institute of Neurobiology, Am Klopferspitz 18, 82152 Martinsried, Germany. E-mail: ikadow@neuro.mpg.de.

DOI:10.1523/JNEUROSCI.2592-11.2011

 0270-6474/11/3115660-14$15.00/0

ity, and thereby suppresses a default CO_2 neuron program in specific MP olfactory sensilla.

Materials and Methods

Fly genetics. Fly stocks were maintained in standard medium at 25°C. The genetic screen was performed with EMS (ethyl methanesulfonate) and eyFLP; FRT/FLP mosaic analysis/mosaic analysis with repressible cell marker (MARCM) analysis, as described previously (Cayirlioglu et al., 2008). The screen resulted in four miR-279-like mutants of ~6000 mutants on the third chromosome that were analyzed. $pros^{IG2227}$ contains a point mutation at Leu850 to Arg. MARCM analysis was performed on flies of either sex of the following genotype: *hsFLP* or *eyFLP; Or-gal4 UAS-sytGFP/+* (or *UAS-mCD8GFP/+*)*; FRT82* mutation/*FRT82 Gal80 (E2F)*. ORN labeling was achieved by fusing the promoter-elements to GAL4 or directly to synaptotagmin-GFP. Mutations included *FRT82B* $miR\text{-}279^{962-7}$ (Cayirlioglu et al., 2008), *FRT82B* $pros^{17}$ (Manning and Doe, 1999), *FRT82B* $pros^{IG2227}$ (this study), and *FRT82B* $pros^{voila78}$ (Grosjean et al., 2001). All analyses were done in mosaic animals. Gr21a transcriptional reporter was used for CO_2 neurons [i.e., *Gr21a-GAL4* driving membrane-bound GFP (*UAS-mCD8GFP*] to detect cell bodies in the antenna and MP. *Elav-GAL4* was used to label neurons. *miR-279-GAL4* contains the 2 kb DNA stretch upstream of *miR-279* gene. As previously described, this driver rescues the mutant phenotype when used to drive the expression of *miR-279* in *miR-279* mutants (Cayirlioglu et al., 2008). *miR-279-GAL4* was used to label cells and progeny of cells expressing *miR-279* in mosaic analysis. Rescue and genetic interaction experiments were performed by using cDNAs fused to UAS transcriptional response elements. UAS-construct expression was under the control of the β-actin promoter, but the expression was restricted to only the mutant tissue in the MP and antenna upon *eyFLP* expression and mitotic recombination. Transgenic flies carrying RNAi constructs were ordered from the VDRC or Kyoto stock centers. RNAi was expressed in exactly the same manner as the UAS constructs in mutant tissue of antenna and MP only. *UAS-Pros* constructs were generated and generously provided by F. Matsuzaki (RIKEN Center for Developmental Biology, Kobe, Japan), C. Doe (Institute of Neuroscience, HHMI, University of Oregon, Eugene, OR), and A. Brand (The Gurdon Institute and Department of Physiology, Development and Neuroscience, University of Cambridge, Cambridge, UK). *UAS-dsred-miR-279* was a gift by E. Lai (Sloan-Kettering Institute, Department of Developmental Biology, New York, NY). *UAS-nerfin* transgenic flies and *nerfin-1* loss-of-function alleles were generously provided by Ward Odenwald (Neural Cell-Fate Determinants Section, NINDS, NIH, Bethesda, MD). *Escargot* loss-of-function and *P*[*lacZ*]*esg* flies were ordered from the Bloomington Stock Center.

Genotypes for analysis. Control:
eyflp;Gr21a-Gal4,UAS-mCD8GFP/+;FRT82/FRT82Gal80E2F
eyflp;Gr21-sytGFP/+;FRT82/FRT82Gal80E2F
eyflp;miR-279-Gal4,UAS-mCD8GFP/+; FRT82/FRT82Gal80E2F
hsflp;Elav-Gal4,UAS-mCD8GFP/+; FRT82/FRT82Gal80
hsflp;miR-279-Gal4,UAS-mCD8GFP/+; FRT82/FRT82Gal80E2F
eyflp;Gr21a-sytGFP actGal4;FRT82/FRT82ClGal80
eyflp;Gr21a-sytGFP actGal4/RNAipros;FRT82/FRT82ClGal80
eyflp;Gr21a-Gal4 UASmCD8GFP/RNAinerfin-1;FRT82/FRT82ClGal80
eyflp;Gr21a-sytGFP actGal4/RNAispineless;FRT82/FRT82ClGal80 (a.o. RNAi constructs against *gcm*, *senseless*, *Ptx1*)
eyflp;Gr21a-Gal4 UASmCD8GFP/escargot^{k00606}*;FRT82 /FRT82ClGal80*
eyflp;Gr21a-Gal4 UASmCD8GFP/+;FRT82 $hb9^{kk30}$*/FRT82ClGal80*
eyflp;Gr21a-Gal4 UASmCD8GFP/+;FRT82 /FRT82ClGal80
eyflp;OrX-Gal4 UASsytGFP/+;FRT82/FRT82ClGal80
eyflp;OrX-Gal4 UASmCD8GFP/+;FRT82/FRT82ClGal80
eyflp;FRT40A/FRT40A GAL80 or *CL;Gr21a-GAL4,UASmCD2*
Mutants:
miR-279, $pros^{IG2227}$, $pros^{Voila78}$, $pros^{17}$
eyflp;Gr21a-Gal4,UAS-mCD8GFP/+;FRT82 mutant/*FRT82Gal80E2F*
eyflp;Gr21-sytGFP/+;FRT82 mutant/*FRT82Gal80E2F*
eyflp;miR-279-Gal4,UAS-mCD8GFP/+;FRT82 mutant/*FRT82Gal80E2F*
hsflp;miR-279-Gal4,UAS-mCD8GFP/+;FRT82 mutant/*FRT82Gal80E2F*
hsflp, Elav-Gal4UASmCD8GFP;FRT82 mutant/*FRT82Gal80*
eyflp;Gr21a-sytGFP actGal4;FRT82 mutant/*FRT82ClGal80*
eyflp;Gr21a-sytGFP actGal4/UASmiR-279 or *UASpros* or *UASnerfin-1; FRT82* mutant/*FRT82ClGal80*
eyflp;Gr21a-sytGFP actGal4/RNAinerfin-1;FRT82 mutant/*FRT82ClGal80*
eyflp;Gr21a-Gal4 UASmCD8GFP/RNAipros;FRT82 mutant/FRT82ClGal80
eyflp;Gr21a-sytGFP actGal4/RNAispineless;FRT82 mutant/*FRT82ClGal80* (*a.o.* RNAi constructs against *gcm*, *senseless*, *Ptx1*)
eyflp;Gr21a-Gal4 UASmCD8GFP/+;FRT82 mutant $hb9^{kk30}$*/FRT82ClGal80*
eyflp;Gr21a-Gal4 UASmCD8GFP/escargot^{k00606}*;FRT82* mutant/FRT82ClGal80
eyflp;Gr21a-Gal4 UASmCD8GFP/+;FRT82 mutant *nerfin159*/FRT82ClGal80
eyflp;OrX-Gal4 UASsytGFP/+;FRT82 mutant/*FRT82ClGal80*
eyflp;OrX-Gal4 UASmCD8GFP/+;FRT82 mutant/*FRT82ClGal80*
eyflp;FRT40A $escargot^{k00606}$*/FRT40A GAL80* or *CL;Gr21a-*GAL4,UASmCD2
eyflp;Gr21a-sytGFP actGal4/UASescargot or *UASnerfin-1* or *UASescargot,* UASnerfin-1;FRT82/FRT82ClGal80
eyflp;Gr21a-sytGFP actGal4/UASp35 or *UAScyclinE;FRT82/* FRT82ClGal80

Tissue dissection and immunohistochemistry. For the analysis of ORN axon targeting in the adult brain, *eyFLP* mosaic flies were dissected and adult brains were fixed and immunostained. For analysis of cell body number and position, *hsFLP* and *eyFLP* were used to create mosaic mutant tissue. Quantifications of ORN number were performed on adult MPs and antennae. Analysis in the developing olfactory neurons was performed using *eyFLP*. White pupae were selected and incubated at 25°C until the desired stage was reached. MPs and antenna regions were dissected in ice-cold PBS and collected in 4% PFA on ice. Upon fixation for 1 h at room temperature (RT) in 4% PFA, tissues were washed twice for 15 min in PBS-0.5% Triton, following by 1 h incubation in blocking solution (20% donkey serum, 0.5% Triton in PBS). Primary antibody was incubated overnight at 4°C in blocking solution without Triton. After washing twice for 15 min in PBS-0.5% Triton, tissues were incubated with secondary antibody for 1 h at RT in blocking solution without Triton. Tissues were washed twice more for 2× 15 min in PBS-0.5% Triton and mounted with Vectashield mounting medium.

All tissues were analyzed using confocal microscopy with an Olympus FV1000 or a Leica SP2 confocal. Pictures were processed in Adobe Photoshop, Adobe Illustrator, ImageJ, and Microsoft PowerPoint.

Primary and secondary antibodies. Staining was performed as previously described (Cayirlioglu et al., 2008). The following primary antibodies were used: chick anti-βgal (1:2000; Abcam); mouse anti-NC82 (1:20), mouse anti-disclarge (1:50), mouse anti-pros (1:20), and mouse and rat anti-elav (1:50) (all from Developmental Studies Hybridoma Bank); and rabbit (1:2000) and mouse (1:500) anti-GFP (both from Clontech). Secondary antibodies (anti-mouse-CY5, anti-rat-CY3, and anti-rabbit-488) were ordered from Dianova and used at 1:200.

Electrophysiology. Extracellular single sensillum recordings from MP were performed according to the procedure described previously (de Bruyne et al., 1999). Briefly, a fly was trapped in a truncated pipette tip with its proboscis protruding out and mounted on a glass slide. The protruding proboscis and MP were secured and stabilized on a coverslip with the help of a tapered glass micropipette. The preparation was visualized with a Leica DM6000 FS microscope at 750× magnification and MP basiconic sensilla were identified by the expression of Gr21a/OrX-GFP in mutant and control flies. A glass reference electrode filled with 0.01 M KCl was inserted into the eye and a recording glass electrode filled with the same solution was used to record from the MP basiconic sensilla. Action potentials were recorded using a CV-7B headstage and MultiClamp 700B amplifier (Molecular Devices). The signals were sampled at 10 kHz, digitized, and fed into a computer by Digidata 1440A. The spikes were visualized and recorded in Clampex 10.2 acquisition software and sorting of spikes were done manually with Clampfit 10.2 software off-line. A continuous and humidified airstream (2000 ml/min) was delivered to the fly throughout the experiment via an 8-mm-diameter glass tube positioned 10 mm away from the preparation. A custom-made odor delivery system was used for stimulation in all experiments (Smartec). For CO_2 stimulation, 500 ms pulses of CO_2 were delivered into the continuous airstream with the help of mass flow controllers and solenoid valves.

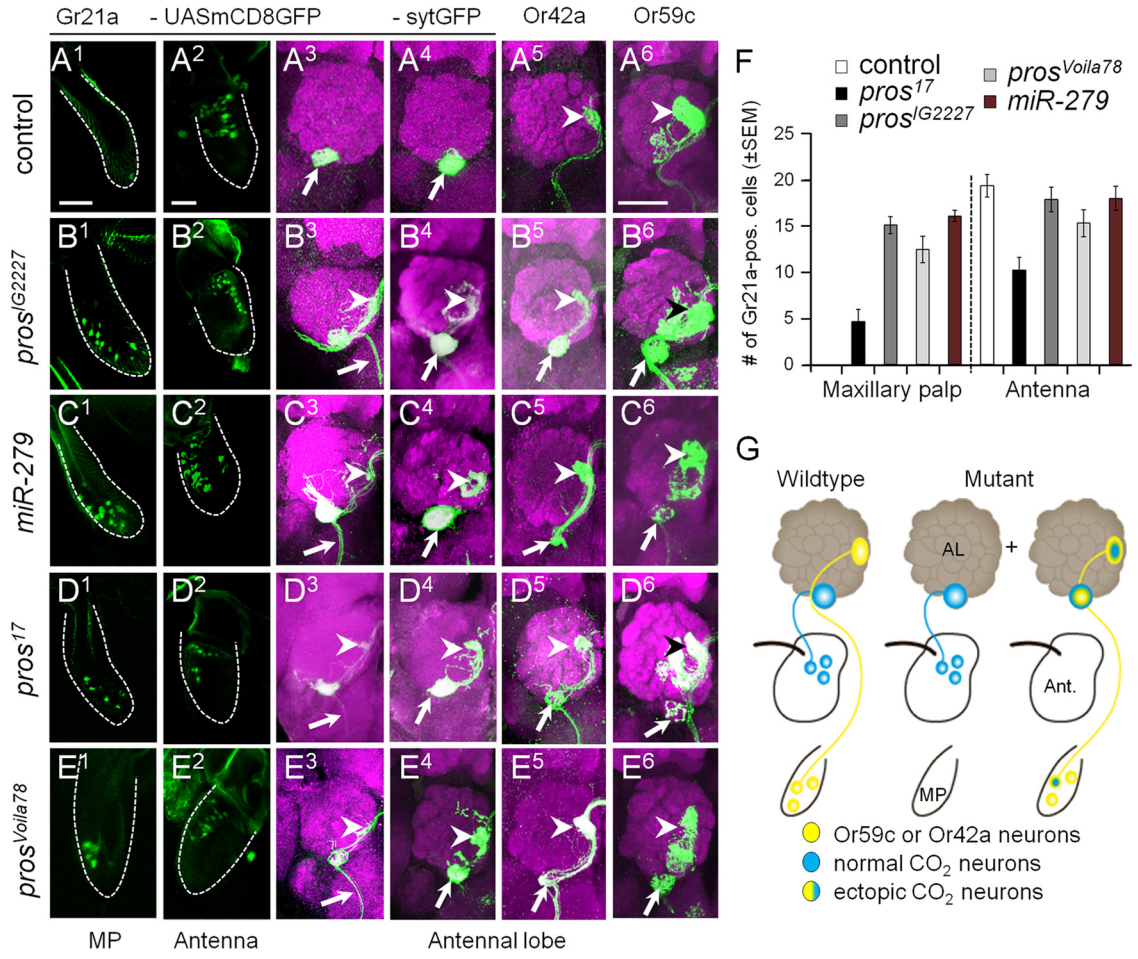

Figure 1. *Pros* mutants exhibit MP CO_2 neurons targeting medial AL glomeruli. ***A–E***, Adult olfactory organs (antenna and MP) and brains stained with anti-GFP (green) or anti-GFP and anti-disc large (magenta) to visualize CO_2 neurons or synaptic projections of CO_2 neurons (*Gr21aGAL4, UAS-sytGFP*) in the AL, respectively. Note that only mutant cells are marked by GFP. ***A*^{1}, ***B*^{1}, ***C*^{1}, ***D*^{1}, ***E*^{1}, CO_2 neurons in MP labeled with *Gr21a-GAL,UAS-mCD8GFP* in control and mutant palps. ***A*^{1}, No CO_2 neurons were detected in MPs of control flies. ***B*^{1}, ***C*^{1}, ***D*^{1}, ***E*^{1}, Ectopic CO_2 neurons were detected in MPs of *eyFLP;pros*^{IG2227}, *eyFLP;pros*^{Voila78}, *eyFLP;miR-279*, and *eyFLP;pros*^{17}. ***A*^{2}, ***B*^{2}, ***C*^{2}, ***D*^{2}, ***E*^{2}, CO_2 neurons in the antenna were labeled with *Gr21a-mCD8GFP*. While CO_2 neuron number appeared normal in *pros*^{IG2227}, *pros*^{Voila78}, and *miR-279* mutants compared with controls, the number was reduced in *eyFLP;pros*^{17} mutants. ***A*^{3}, AL of *eyFLP;FRT82B* control fly, where CO_2 neurons target a single glomerulus, V-glomerulus. ***B*^{3}, ***C*^{3}, ***D*^{3}, ***E*^{3}, CO_2 neurons labeled with Gr21a-mCD8GFP innervate medial glomeruli (arrowhead) in addition to the V-glomerulus in brains of *eyFLP;pros*^{IG2227}, *eyFLP;pros*^{Voila78}, *eyFLP;miR-279*, and *eyFLP;pros*^{17} flies. Note that CO_2 neuron axons project via the labial (arrow) and via the antennal nerve to the V-glomerulus and to medial glomeruli. Axons form contralateral projections. ***A*^{4}, ***B*^{4}, ***C*^{4}, ***D*^{4}, ***E*^{4}, Similar scenario as in ***A*^{3}, ***B*^{3}, ***C*^{3}, ***D*^{3}, and ***E*^{3}; however, here CO_2 neurons are labeled with Gr21a-sytGFP to label synaptic connections in the AL. ***A*^{5}, ***B*^{5}, ***C*^{5}, ***D*^{5}, ***E*^{5}, ORNs expressing the Or42a receptor residing on MPs innervate a medial glomerulus (arrowhead) in the AL of *eyflp;FRT82B* controls (***A*^{5}). ***B*^{5}, ***C*^{5}, ***D*^{5}, ***E*^{5}, Or42a neurons in *eyFLP;pros*^{IG2227}, *eyFLP;pros*^{Voila78}, *eyFLP;miR-279*, and *eyFLP;pros*^{17} target the V-glomerulus (arrow) in addition to the medial glomerulus. ***A*^{6}, ***B*^{6}, ***C*^{6}, ***D*^{6}, ***E*^{6}, Or59c neurons reside on the MP. Note that these neurons show the same behavior as Or42a neurons in control and mutants. ***F***, Quantification of CO_2 neurons of antenna and MP for all flies analyzed. Control: $n = 15$ and 11, *pros*^{17}: $n = 17$ and 45 (8 with ectopic CO_2 ORNs), *pros*^{IG2227}: $n = 51$ and 7, *miR-279*: $n = 37$ and 6, *Pros*^{Voila78}: $n = 9$ and 10, for antenna and MP, respectively. Control versus *pros*^{Voila78} antenna, $p = 0.07$; control versus *pros*^{17} antenna, $p = 0.005$; *pros*^{Voila78} versus *pros*^{IG2227} antenna, $p =$ n.s.; *miR-279* versus *pros*^{IG2227} MP, $p =$ n.s.; *pros*^{17} versus *pros*^{IG2227} MP, $p < 0.001$. ***G***, Schematic representation of CO_2 neuron projections in wild-type and mutant flies. Ectopic CO_2/MP hybrid neurons are detected in the MPs of *miR-279* and *pros* mutants. While the mutant CO_2 neurons in the antenna show wild-type innervations of the AL (blue), mutant axons from the MP innervate the V-glomerulus and additional medial glomeruli and express the CO_2 receptors and MP ORs (yellow-blue). MP neurons innervate via the labial nerve in both mutants and wild-type flies (yellow). Ant, antenna; pos., positive. Scale bars, 50 μm.

For odor stimulation, specific odors were diluted 1:10 in paraffin oil and 300 ml/min odor pulse were delivered into the continuous airstream using headspace method. During the odor stimulation, the continuous airstream flow was maintained always at 2000 ml/min with the help of mass flow controllers and solenoid valves. The spikes in the recorded traces were sorted according to spike amplitude. The spike quantification was done by counting the number of spikes over 500 ms duration immediately after the onset of the response and subtracting the total from the number of spikes counted over a 500 ms window before the stimulation. The obtained number of spikes were doubled and presented as spikes per second.

Bioinformatic binding site predictions. The presence of the Prospero binding motifs TWAGVYD (Cook et al., 2003) or CWYNNCY (Choksi et al., 2006) in the 2 kb upstream region of the *miR-279* gene was tested using the RSA tools software (http://rsat.ulb.ac.be/genome-scale-dna-pattern_form.cgi). The predicted putative binding sites were further evaluated by testing the conservation in six different *Drosophila* species (*D. melanogaster*, *D. yakuba*, *D. simulans*, *D. erecta*, *D. ananassae*, *D. pseudoobscura*) using the VISTA genome browser (http://pipeline.lbl.gov/cgi-bin/gateway2).

Promoter S2 cell assay. The genomic 2 kb upstream region of *miR-279* was amplified and cloned into the pGL3 vector. This putative enhancer region was further mutagenized at the predicted conserved Prospero binding sites using the Stratagene QuikChange Lightning Multi Site-Directed Mutagenesis Kit. The following primers were used to perform the nucleotide exchange: mutP1 forward: acagttcaaatgtgccgtctaatttctaatgatttaatttc; mutP2 forward: gcgcgtgtgtaagacgttgattgttagtgtacgg; mutP3 forward: cctggtacaatgaagattcgcatttagaataaggca; and mutP4 forward: gggaggaaagcattcacagacaacaacccttctggg.

S2 cells were transfected with a reporter construct carrying either the wild-type enhancer fragment or a construct with mutations at four putative and conserved Prospero binding sites. For normalization, the pTK Renilla

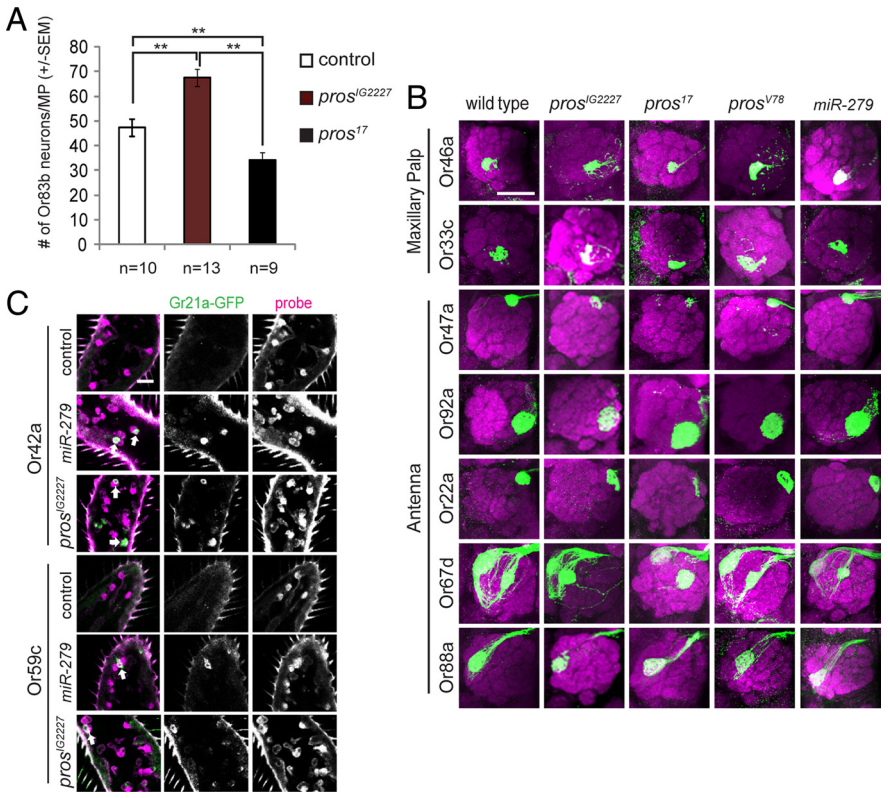

Figure 2. Analysis of *pros* and *miR-279* mutants reveals specific and general effects on ORN number and targeting. ***A***, MP ORNs were quantified using the general OR marker Or83b-GFP (*Or83b-GAL4, UAS-mCD8GFP*). The number of ORNs in $pros^{IG2227}$ clones was increased compared with control clones. This increase correlated with the number of ectopic CO_2 neurons in the mutants. The number of ORNs in $pros^{17}$ clones was decreased by ~10 ORNs on average compared with control clones. ***B***, eyFLP mosaic analysis was used to analyze ORN projection patterns in the AL of several classes of ORNs. *miR-279* and *pros* mutants show very mild mistargeting in few classes of non-CO_2 receptor ORNs. In general, mistargeting was mild and random. *Pros* mutants display a reduction of Or22a and Or47a neurons, as shown by the reduced innervations of the AL glomerulus. ***C***, Ectopic CO_2 neurons on the MP coexpress Or42a and Or59c. Examples of whole-mount *in situ* hybridization on control and mutant MP clones expressing the Gr21a-mCD8GFP reporter are shown. Scale bars: ***B***, 50 μm; ***C***, 10 μm.

vector that expresses the Renilla luciferase was cotransfected. Both vectors were used in a concentration of 100 ng. The cells were seeded in a density of 10^6 cells and transfected the next day with the constructs described. Approximately 16 h after transfection, the cells were lysed and luciferase expression assayed using the dual luciferase kit (Promega) according to the manufacturer's instructions. For overexpression of Pros, a full-length EST (LD37627; Berkeley Drosophila Genome Project) was subcloned into the pattBUAS vector (donated by the Basler Lab, Institute of Molecular Life Science, University of Zurich, Zurich, Switzerland). The RNAi pros construct was a gift from the VDRC library (Construct ID: 109284). To drive the expression of both constructs, ubiquitinGal4 was cotransfected. All experiments were performed in triplicates.

Electromobility shift assay. For the electromobility shift assay, the homeodomain of Pros was purified from BL21 cells transfected with the construct pGex-prosL that was kindly provided by Tiffany Cook (Department of Pediatric Ophthalmology, Division of Developmental Biology, Cincinnati Children's Hospital Medical Center, Cincinnati, OH). Oligos containing the predicted Prospero binding sites, as follows, were annealed and radiolabeled with [γ ^{32}P] ATP using T4 polynucleotide kinase (Fermentas): P1 forward: gatgcaagcagcatttacagttcaaatgtgccgtctaattagaaatgatt taatttcaat; mutP1 forward: gatgcaagcagcatttacagttcaaatgtgccgtctaatttctaat gatttaatttcaat; P4 forward: gagggtagcgcaaggaaaggggaggaaagctaagacagacaa caaccttctggg; and mutP4 forward: gagggtagcgcaaggaaaggggaggaaagca ttcacagacaacaacccttctggg.

The labeled oligos were mixed with the purified proteins in binding buffer (20 mM HEPES, pH 7.5, 100 mM NaCl, 1 mM DTT, 5 mM $MgCl_2$) and incubated for 20 min at RT. Subsequently, the mixture was loaded on a 0.5% Tris-borate/EDTA prerun minigel. The gel was dried and exposed to a Phospho screen overnight.

Chromatin immunoprecipitation assay. Embryos (UAS-Flag-Pros/X; actin-Gal4/+) were collected and fixed as previously described (Sandmann et al., 2006). The embryos were fixed in a cross-linking solution (50 mM HEPES, 1 mM EDTA, 0.5 mM EGTA, 100 mM NaCl, pH 8.0) for 15 min under vigorous shaking. The cross-linking reaction was stopped by adding PBS with 125 mM glycine and 0.1% Triton-X. Embryos were washed twice with PBT (0.1% Triton-X), dried, and frozen in −80°C. For cell lysis, embryos were homogenized in PBS with 0.1% Triton-X and protease inhibitor, centrifuged, and the pellet dissolved in cell lysis buffer (5 mM HEPES, pH 8.0, 85 mM KCl, 0.5% NP-40 and protease inhibitor). After the centrifugation, the pellet was dissolved in nuclear lysis buffer (50 mM HEPES, pH 8.0, 10 mM EDTA, 0.5% *N*-lauroylsarcosine and protease inhibitor) and incubated at room temperature for 20 min. Lysates were sonicated (Sonicator sonoplus; Bandelin) until an approximate chromatin fragment length of 1000–500 bp was achieved. The sheared chromatin fragments were incubated overnight with magnetic beads and anti-FLAG M2 (Sigma) to detect Flag-Pros or mouse IgG as unspecific binding control. Beads were washed and the bound chromatin was eluted according to the manufacturer's instructions (Magna ChIP G Kit; Millipore). The chromatin was checked for the presence of miR-279 promoter fragments by PCR using the following primer sets: chromatin immunoprecipitation assay (ChIP) P4 forward: gtatataatggacaagaagaagaataagcag; ChIP P4 reverse: catgcggaatttcagttgtttccttttatatc. An input control was included into the PCR.

3′UTR S2 cell assay. To generate luciferase targets, we amplified a 1.8 kb *nerfin* fragment (including the entire 3′UTR and 220 bp of downstream sequence), and a 644 bp *escargot* 3′UTR fragment and cloned these downstream of the renilla luciferase coding region in psiCHECK2; this vector contains an internal firefly luciferase gene that serves as an internal control. For the *miR-279* expression construct, we cloned 415 bp of genomic sequence, centered on the *miR-279* hairpin, into the 3′UTR of UAS-DsRed vector. We then transfected 100 ng of target, 50 ng of ub-Gal4, and 100 ng of UAS-DsRed-miR-279 plasmids into 1×10^6 S2 cells in 24-well format. Three days later, we lysed the cells and subjected them to dual luciferase assay (Promega) and analyzed these on a plate luminometer (Tecan). Triplicate transfections were performed. Data of four repetitions were pooled (Fig. 9).

Gene ontology term analysis and miR-279 target prediction software. Prospero *in vivo* target genes were previously published (Choksi et al., 2006). *microRNA-279* target gene predictions were generated with the following online software: TargetScan (http://www.targetscan.org/fly_12/), PicTar (http://pictar.mdc-berlin.de/cgi-bin/new_PicTar_fly.cgi?species=fly), and miRBase (http://www.mirbase.org/). Only targets that appeared in at least two of the predictions were used for the comparison to the list of Prospero target genes. Gene ontology (GO) analysis was performed using GOstat (Beissbarth and Speed, 2004). All predictions were Benjamini-corrected and GO terms with a $p > 0.01$ were disregarded. Targets for *aga-miR-279* were predicted using miRBase. Results can be found at http://www.ebi.ac.uk/enright-srv/microcosm/cgi-bin/targets/v5/hit_list.pl?genome_id=377&mirna_id=aga-miR-279&external_name=&gene_id=&go_class=function&go_term=&logic=phrase&terms=. *aga-nerfin-1* is AGAP002601 and *aga-escargot* is AGAP008274.

Table 1. Quantification of ORN mistargeting phenotypes

ORN	Wild-type	$pros^{IG2227}$	$pros^{17}$	$pros^{Voila78}$	*miR-279*
59c	0/11 (0%)	12/17 (71%)	4/35 (11%)	30/30 (100%)	10/12 (83%)
42a	0/9 (0%)	4/5 (80%)	7/19 (37%)	8/11 (73%)	18/24 (75%)
46a	0/19 (0%)	0/4 (0%)	0/20 (0%)	2/25 (8%)	0/25 (0%)
33c	0/19 (0%)	0/20 (0%)	0/14 (0%)	4/4 (100%)	0/6 (0%)
47a	0/12 (0%)	0/12 (0%)	0/5 (0%)	0/10 (0%)	0/9 (0%)
92a	0/17 (0%)	0/12 (0%)	0/14 (0%)	0/14 (0%)	0/33 (0%)
22a	0/24 (0%)	0/21 (0%)	0/20 (0%)	0/30 (0%)	0/23 (0%)
67d	0/11 (0%)	13/26 (50%)	0/12 (0%)	0/22 (0%)	0/40 (0%)
88a	0/24 (0%)	0/19 (0%)	0/20 (0%)	18/44 (41%)	0/11 (0%)

Brains of *pros* and *miR-279* mutants were analyzed with eyFLP and mosaic labeling. Representative images are shown in Figures 1 and 2.

Results

Pros mutants fail to suppress the formation of maxillary palp CO_2 neurons

miR-279 activity suppresses the formation of CO_2 sensory neurons in the MPs of *D. melanogaster* (Cayirlioglu et al., 2008). To gain insight into the relationship of *miR-279* and regulators of neuron development, we used genetic mosaic screening to identify mutations with a *miR-279*-like phenotype. We identified a new allele of Pros, $pros^{IG2227}$, which strongly resembled the phenotype of *miR-279* mutants and displayed a similar number of ectopic CO_2 neurons on the MP (15 ± 0.9 for $pros^{IG2227}$ and 16 ± 0.6 for *miR-279*; Fig. 1A^1, B^1, C^1,F). The number of antennal CO_2 neurons in $pros^{IG2227}$ and *miR-279* mutants was not affected and comparable to controls (18 ± 3.2 and 18 ± 3.5 vs 19.4 ± 4, respectively; Fig. 1A^2, B^2, C^2,F). Antennal CO_2 ORNs target the V-glomerulus in the AL of the adult fly brain (Fig. 1A^3,A^4). In $pros^{IG2227}$ and *miR-279* mutants, axons of ectopic MP Gr21a-expressing neurons showed dual targeting specificity. In addition to targeting the V-glomerulus, these neurons innervated a set of medial glomeruli usually innervated by two MP ORN classes, Or42a and Or59c (Fig. 1B^3, B^4, C^3, C^4).

Next, we asked how $pros^{IG2227}$ relates to previously published alleles of *pros*. It was previously reported that full loss of *pros* resulted in a partial conversion of the neural to the non-neural cell lineage and, consequently, in a loss of neurons (Manning and Doe, 1999; Reddy and Rodrigues, 1999; Sen et al., 2003). Consistent with these results, $pros^{17}$ mutants exhibited ORN number reduction as revealed by the general OR marker Or83b-GFP (*Or83b-Gal4,UAS-mCD8GFP*) and sparser innervations of a subset of AL glomeruli (Fig. 2A,B). $pros^{17}$ flies also displayed a loss of antennal CO_2 neurons to 51.5% of controls (10 ± 1.3 and 19.4 ± 4; Fig. 1D^2,F). Nevertheless, $pros^{17}$ mutant MPs displayed ectopic CO_2 neurons in 17% (4.6 ± 1.4) of flies analyzed (Fig. 1D^1,F). These 17% displayed medial mistargeting as *miR-279* and $pros^{IG2227}$ mutants (Fig. 1D^3–D^4). Another previously published hypomorphic P-element excision, $pros^{Voila78}$ (Grosjean et al., 2001), showed a phenotype reminiscent of the $pros^{IG2227}$ phenotype (Fig. 1E^1–E^4,F).

To address whether the phenotype of the hypomorphic alleles of *pros* is restricted to the formation of ectopic CO_2 ORNs as it is in *miR-279* mutants, we next analyzed the projection patterns of several antennal and MP ORNs. $pros^{IG2227}$ and $pros^{Voila78}$ again displayed a similar selectivity as *miR-279* mutants (Figs. 1, 2, Table 1, and data not shown). As previously reported for *miR-279* mutants, two types of MP ORNs, Or59c and Or42a, target the V-glomerulus, in addition to innervating medial glomeruli in all mutants (Fig. 1A^5, A^6, B^5, B^6, C^5, C^6, D^5, D^6, E^5, E^6). This mistargeting corresponds to the coexpression of either Or59c or Or42a in ectopic MP CO_2 neurons, as shown by *in situ* hybridization against Or42a or Or59c mRNA in mutant and wild-type MPs (Fig. 2C).

We tested the functionality of the ectopic CO_2/Or59c or Or42a hybrid neurons using single sensillum recordings (Fig. 3).

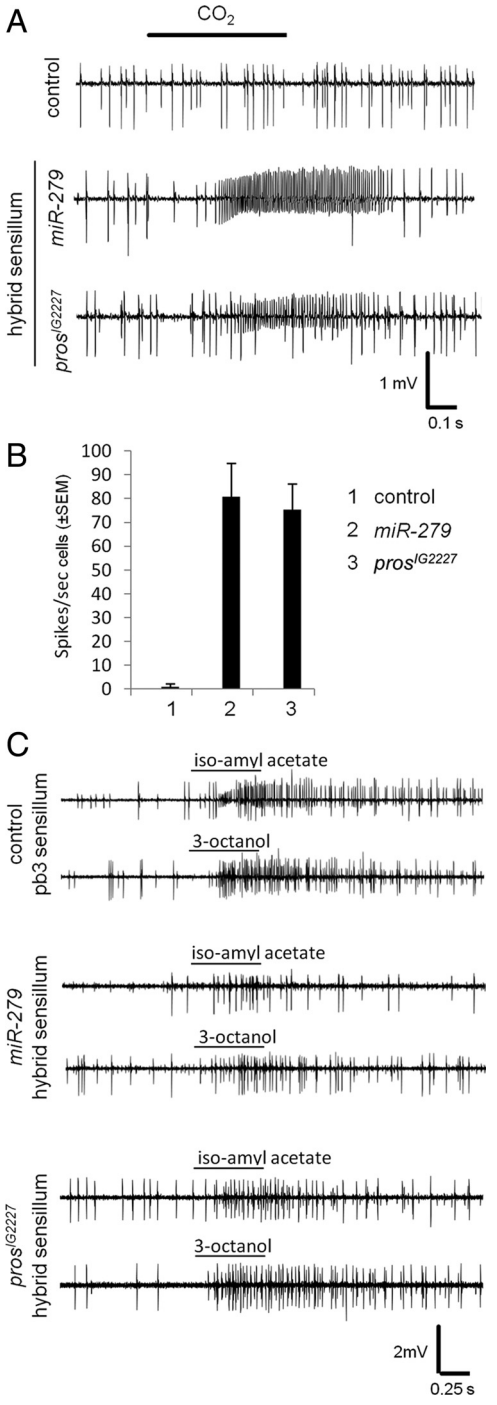

Figure 3. Hybrid neurons respond to CO_2 and MP key odors. ***A***, Representative single sensillum recording traces from the MP basiconic sensilla of control, *miR-279*, and $pros^{IG2227}$ flies. Control trace (top) shows spikes of two neurons. In both *miR-279* (middle) and $pros^{IG2227}$ (bottom) traces, spikes of an extra neuron are visible. During a 500 ms CO_2 stimulation (black bar), the spike frequency of the B neuron in both *miR-279* and $pros^{IG2227}$ increased significantly. No response was observed in control MPs. ***B***, Spike frequency of B neurons to CO_2 stimulation in control, *miR-279*, and $pros^{IG2227}$ flies are represented in the graph ($n = 10$ recordings for each genotype, ±SEM). ***C***, Representative single sensillum recording traces from the MP basiconic sensilla of control ($n = 5$), *miR-279* ($n = 6$), and $pros^{IG2227}$ ($n = 6$) flies stimulated with two key ligands of pb3 sensilla, iso-amyl acetate, and 3-octanol.

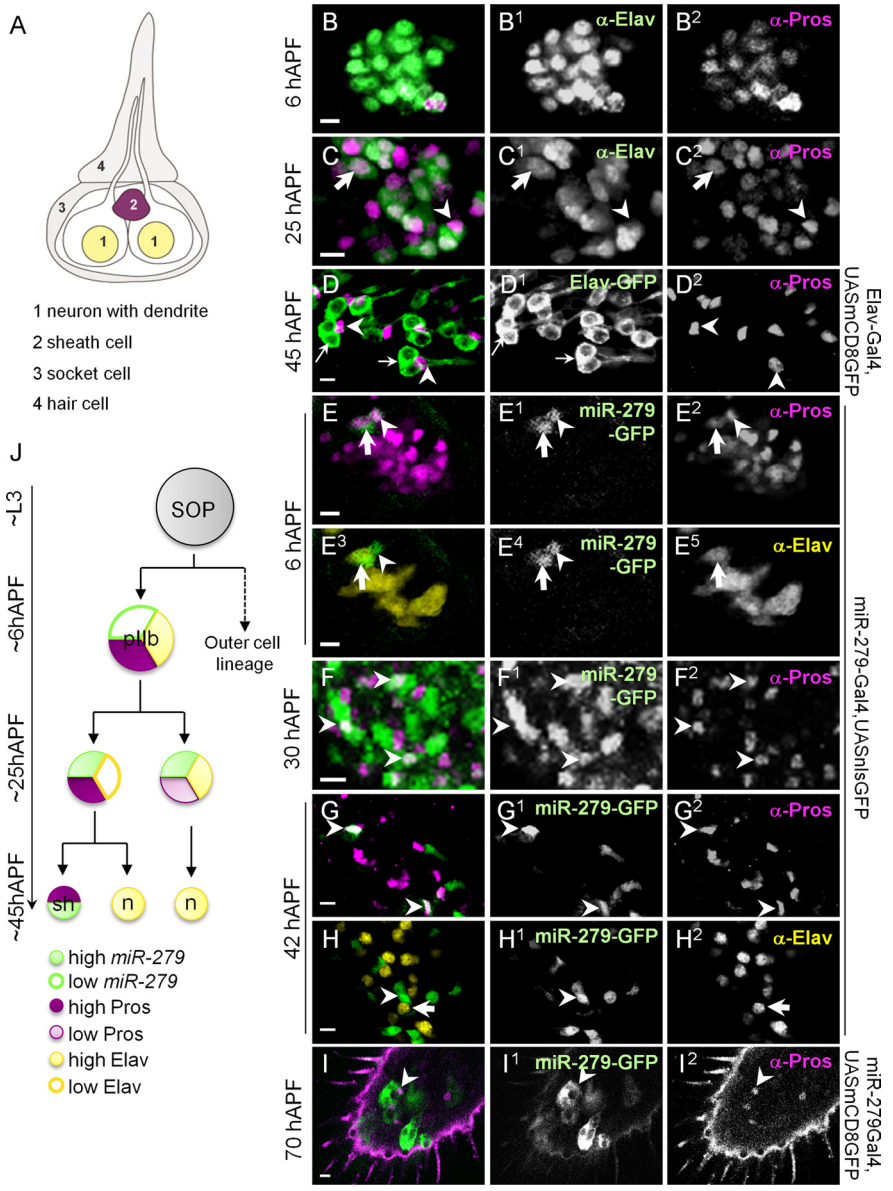

Figure 4. Prospero and *miR-279* are coexpressed in the MP. ***A***, Schematic drawing of a fully differentiated wild-type MP sensillum with two neurons. ***B***, Developing MP at 6 h APF stained with anti-Elav (green, ***B*^{1}**) and anti-Pros (pink, ***B*^{2}**). Note the almost complete overlap of expression. ***C***, Developing MP at 25 h APF stained with anti-Elav (***C*^{1}**) and anti-Pros (***C*^{2}**). Low and high Pros-expressing cells are indicated with arrow and arrowhead, respectively. Cells with low Pros expression seem to also express Elav. ***D***, MP of *elav-GAL4,UAS-mCD8GFP* fly at 45 h APF stained with anti-GFP (***D*^{1}**) and anti-Pros (***D*^{2}**). Elav-positive cells (arrow) do not express Pros anymore. Two Elav-expressing cells are located next to one Pros-expressing cell (arrowhead). ***E***, Developing MP of *miR-279-Gal4,UAS-nlsGFP* at 6 h APF stained with anti-GFP (***E*^{1}** and ***E*^{4}**), anti-Elav (***E*^{5}**), and anti-Pros (***E*^{2}**). *miR-279* starts to be expressed and colabels with Pros (arrow and arrowhead). The weaker Pros-positive cell is also Elav-positive (arrow). ***F***, Developing MP of *miR-279-GAL4,UAS-mCD8GFP* at 30 h APF stained with anti-GFP (***F*^{1}**) and anti-Pros (***F*^{2}**). Many cells express miR-279-GFP, some of which are also Pros-positive (arrowheads) ***G***, MP from *miR-279-GAL4,UAS-nlsGFP* at 42 h APF stained with anti-GFP (***G*^{1}**) and anti-Pros (***G*^{2}**). *miR-279* remains coexpressed with Pros (arrowhead) in some cells. ***H***, MP from *miR-279-GAL4,UAS-nlsGFP* at 42 h APF stained with anti-GFP (***H*^{1}**) and anti-Elav (***H*^{2}**) *miR-279*-positive cells (arrowhead) do not colabel with Elav (arrow). ***I***, MP, *miR-279-GAL4,UAS-mCD8GFP* in an *eyFLP* control clone at 70 h APF stained with anti-GFP (***I*^{1}**) and anti-Prospero (***I*^{2}**). Arrowhead shows a *miR-279*-positive cell, which is expressing Pros. ***J***, Model of the divisions of the cells of the inner (pIIb) lineage. Respective expression of Pros, Elav, and *miR-279* are indicated. SOP, Sensory organ precursors; n, neuron; sh, sheath cell; L3, larval stage 3. Scale bars, 5 μm.

Ectopic MP CO_2 neurons on *miR-279* and *pros*^{IG2227} mutant palps were functional and responded to CO_2 (Fig. 3*A*,*B*). In addition, sensilla containing ectopic CO_2 hybrid neurons also responded to Or42a and Or59c specific odors such as iso-amyl acetate and 3-octanol, in line with their receptor expression profile (Fig. 3*C* and data not shown) (de Bruyne et al., 1999). Thus, CO_2 neurons are formed within Or42a and Or59c sensilla, and coexpress and respond to either of these receptors.

In summary, mutations in Pros in the olfactory lineage result in the selective formation of ectopic MP CO_2 hybrid neurons, as previously reported for *miR-279* mutants. Complete lack of Pros also frequently displayed a less ORN-specific and more severe phenotype of neuron loss, including antennal CO_2 neurons, comparable to previous reports in ES organs and antenna. These results suggest that Pros, in addition to its early function in pIIb versus pIIa specification, also restricts neuron formation in specific MP olfactory sensilla.

Pros is expressed in the olfactory lineage and maintained in mature sheath cells

The similarity of *pros* and *miR-279* mutant phenotypes suggest that Pros and *miR-279* act on the same developmental mechanism and potentially same genetic network. We next asked whether Pros and *miR-279* are coexpressed during olfactory system formation. The MP develops during pupal life from a cluster of sensory organ precursors in the antennal part of the eye-antennal imaginal disc (Lebreton et al., 2008). In the mature wild-type MP, every olfactory sensillum contains two ORNs, one sheath, one socket, and one shaft cell (Fig. 4*A*). In the developing MP, the neural marker Elav was first detected using an anti-Elav antibody at ~6 h after puparium formation (APF). At this time point, Elav staining overlapped with staining against Pros (Fig. 4*B*). Two populations stained at different intensities with Pros coexpressed Elav. At 25 h APF, Elav-only cells and Pros-only cells were present next to cells with low levels of Pros that coexpressed high Elav, and vice versa (Fig. 4*C*). At 45 h APF, Elav and Pros were completely separated, and the final sensillum composition was defined. Two neurons expressed Elav and, conversely, Pros became restricted to the sheath cell (Fig. 4*D*). These stainings and additional markers are consistent with previous observations (Manning and Doe, 1999), where Elav and Pros are coexpressed early on in the neural lineage pIIb cell (Fig. 4*J*). The pIIb cell divides and gives rise to a pIIIb and a pIIIb* cell that can be distinguished by their high versus low levels of Pros. Finally, the high Pros-expressing cell divides again and produces a Pros-positive sheath cell and a Pros-negative neuron, whereas the cell with lower Pros levels gives rise to a single neuron (Fig. 4*J*).

Next, we used an enhancer element (2 kb upstream of the *miR-279* gene), which was sufficient to rescue the phenotype in

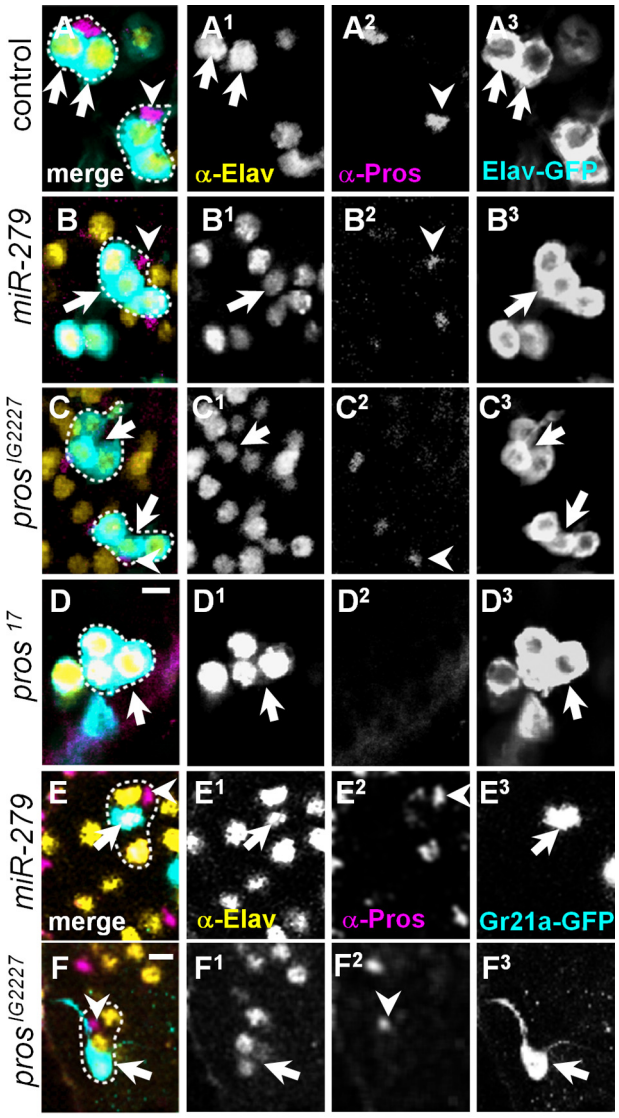

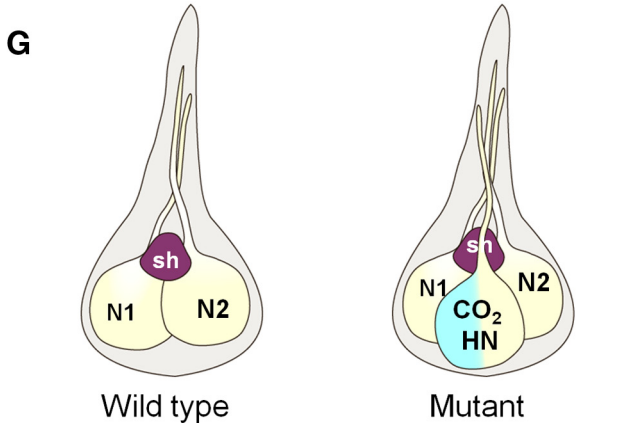

Figure 5. Pros and *miR-279* suppress CO_2 neuron formation in MP sensilla. ***A–F***, MPs at 45 h APF (***A–D***) or pharate adults (***E***, ***F***), stained with anti-GFP (turquoise), anti-Elav (yellow), and anti-Pros (pink). Cells belonging to one sensillum are circled with a dashed line. ***A***, Wild-type showing two *Elav-GAL4*-positive cells (arrows, A^3) costained with anti-Elav (arrows, A^1) and one adjacent Pros-expressing cell (arrowhead, A^2). ***B***, *miR-279* MP clone (circled area) showing three Elav-GFP cells (arrow, B^3), which are positive for Elav (arrows, B^1). Pros-positive cell is seen next to the cluster (arrowhead). ***C***, Two examples of $pros^{IG2227}$ clones (circled areas) with three neurons positive for Elav (arrows, C^1). Notably, Pros labeling is reduced compared with wild-type clones (arrowhead, C^2). ***D***, Similar example of a $pros^{17}$ clone of three *Elav-GAL4*-positive cells (arrow). The adjacent neurons outside the circled area belong to different sensilla in close vicinity. Pros expression is not detectable in $pros^{17}$-null mutant. ***E***, *miR-279* clone with single Gr21a-positive cell (arrow, E^3), which costains with anti-Elav (arrow, E^1) but not anti-Pros (arrowhead, E^2). ***F***, Similar example of a $pros^{IG2227}$ clone with a GR21a-positive cell (arrow, F^3), which is positive for anti-Elav (arrow, F^1). ***G***, Schematic model of wild-type sensillum housing two neurons (N1 and N2) and one sheath cell (sh). Mutant sensillum with three neurons and one sheath cell is depicted. The additional neuron is a hybrid neuron (HN) and expresses the CO_2 receptors and either Or42a or 59c. Scale bars, 5 μm.

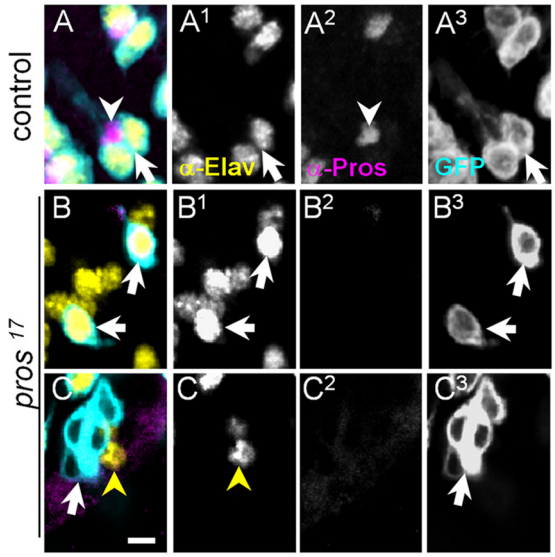

D	Phenotype in maxillary palp		
	ectopic neuron	pIIb to pIIa conversion	
genotype	3-neuron sensillum	1-neuron sensillum	undiff. neuron
WT	0 %	0 %	0 %
$pros^{IG2227}$	100 %	10 %	0 %
miR-279	100 %	4 %	0 %
$pros^{17}$	54 %	31 %	15.5 %

Figure 6. Pros and *miR-279* define olfactory neuron number. MPs at 45 h APF stained with anti-GFP (turquoise), anti-Elav (yellow), and anti-Pros (pink). ***A***, In wild-type sensilla, two *Elav-GAL4*-positive cells costain with anti-Elav (arrows) and one Pros-expressing cell resides next to them (arrowhead). ***B***, $pros^{17}$ clone with single Elav-positive cells (arrows). Pros expression is not detectable in the $pros^{17}$-null mutation. ***C***, $pros^{17}$ clones of *Elav-GAL4*-positive cells (arrow), which failed to maintain the expression of Elav protein. ***D***, Pros activity is required at distinct steps during lineage formation. $pros^{17}$ mutants show an early phenotype during pIIb to pIIa specification. The pIIb lineage partly converts to the pIIa lineage in these mutants. This results in a partial or complete loss of ORNs, giving rise to sensilla with only one neuron (31%) or clusters of undifferentiated (undiff.) cells (15.5%). These scenarios are also seen rarely in $pros^{IG2227}$ (10%) and *miR-279* mutants (4%). n ($pros^{17}$) = 13, n ($pros^{IG2227}$) = 19, and n (*miR-279*) = 22 MPs. Hypomorphic alleles of $pros^{IG2227}$ and $pros^{Voila78}$ uncover a second phase of Pros requirement during definition of sensilla neuron number. In these mutant palps and in 54% of $pros^{17}$ mutant palps, a third neuron was formed within a sensillum. This neuron expressed Gr21a receptor (CO_2 receptor) starting at late pupal stages. While Pros is involved in pIIb versus pIIa specification, *miR-279* is specifically required downstream of Pros within the already determined neuronal lineage to define the number of ORNs in certain MP sensilla. Scale bars, 5 μm.

miR-279 loss-of-function mutants to analyze *miR-279* expression (Cayirlioglu et al., 2008). miR-279-GFP (*miR-279-GAL4*, *UAS-mCD8-GFP/-nls-GFP*) was first detected in MP precursor cells in the eye–antennal disc at 6 h APF (Fig. 4E^1,E^4). At this time, both

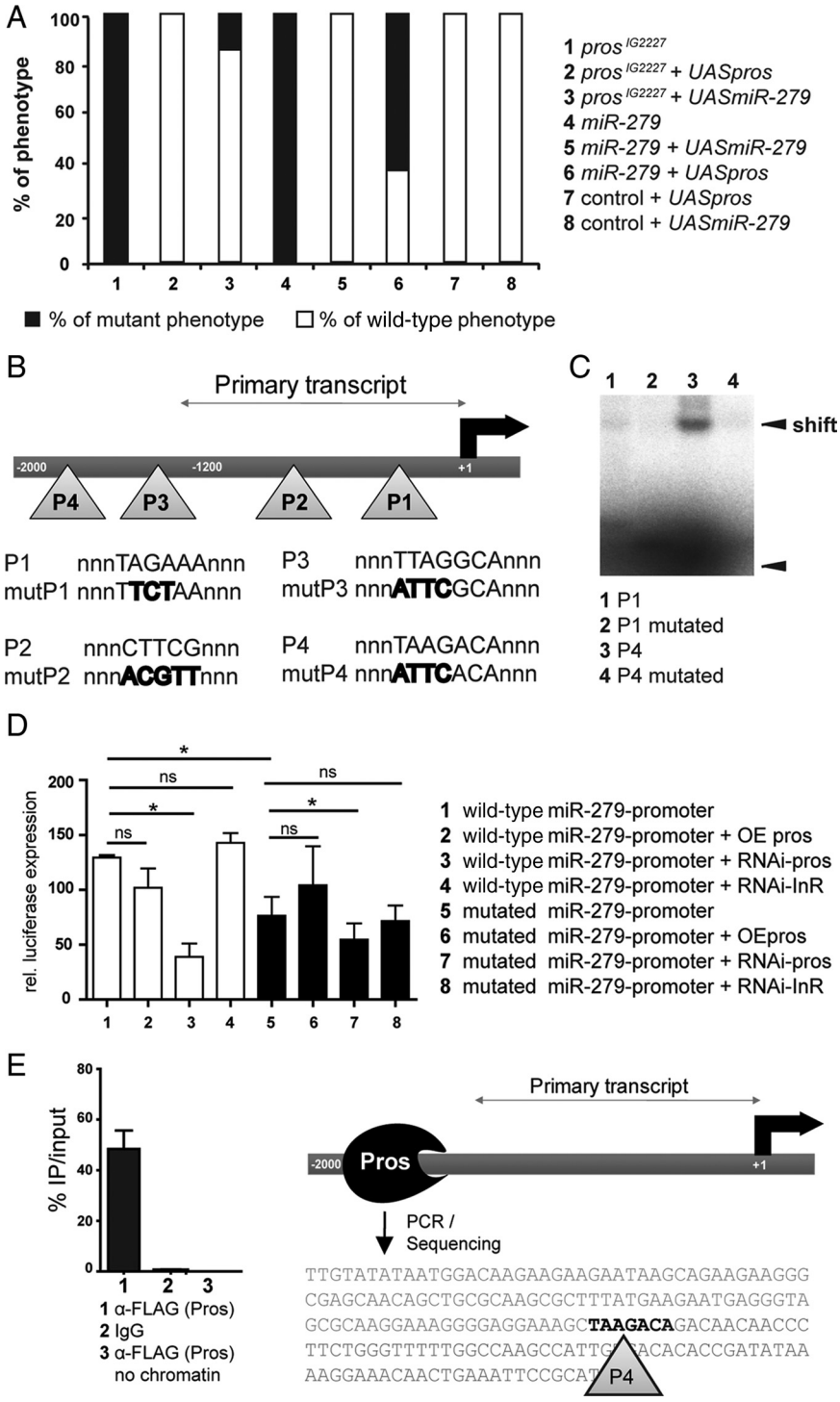

Figure 7. *miR-279* and Pros interact *in vitro* and *in vivo*. ***A***, Expression of *UAS-pros* as well as *UAS-miR-279* in the *eyFLP;pros*^{IG2227} mutant background rescued the phenotype almost fully (100%, $n = 25$ and 80%, $n = 81$, respectively), while expression of *UAS-pros* in the *eyFLP;miR-279* mutant background only led to a partial rescue of 37% ($n = 25$). Overexpression of Pros or *miR-279* in wild-type clones did not result in a detectable phenotype in Gr21a-expressing neurons ($n = 20$). ***B***, Scheme of the putative enhancer region of *miR-279* depicting the relative positions of the predicted Pros binding sites (P1–P4). The binding sites include either the consensus motif TWAGVYD or CWYNNCY. The primary transcript starts ~1200 bp upstream of *miR-279*. Sequences of putative binding sites and sequences of mutated sites within the consensus sequence are shown. ***C***, Gel shift assay using purified homeodomain of Pros. Radiolabeled oligos carrying either P1 or P4 sites were assayed for direct Pros binding. Pros homeodomain binds to P4, which results in a strong shift (lane 3). The shift is strongly reduced when mutated P4 oligos were tested (lane 4). ***D***, S2 cell *miR-279* promoter reporter assays with wild-type and mutated versions of the promoter. Note that RNAi against Pros strongly reduced *miR-279* reporter expression, while Pros overexpression did not significantly enhance reporter expression of the wild-type and mutated promoter constructs (*$p < 0.05$). ***E***, Quantification of percentage PCR product of immunoprecipitated (IP) chromatin compared with the input. Anti-FLAG to pull down Pros-FLAG was compared with mouse IgG plus chromatin and anti-FLAG antibody without chromatin. The PCR was conducted with a primer set amplifying the region around P4. The sequence of the PCR product is shown.

Elav and Pros expression was significantly broader than miR-279-GFP expression, but all *miR-279*-positive cells were also positive for Pros or Pros/Elav staining (Fig. 4*E*,*E*^{3}). By 30 h APF, we detected a large number of miR-279-GFP cells, and the overlap with Pros staining was still high (Fig. 4*F*). At 42 h APF, expression became more defined and overall dropped to fewer cells compared with 30 h APF (Fig. 4*G*,*H*). While the overlap with Pros remained significant, we did not detect any *miR-279*-cells positive for the neuronal marker Elav (Fig. 4*H*). In MPs analyzed at 70 h APF, Pros and *miR-279* were confined to sheath cells (Fig. 4*I*).

These data demonstrate that the first *miR-279*-expressing cells are also positive for Pros. While both Pros and *miR-279* initially overlap with the neuronal marker Elav, in midpupal stages when most of the sensory cells have been determined, Pros and *miR-279* are excluded from neurons. In the mature MP, Pros and *miR-279* are expressed in the sheath cell. While Pros expression is detected early in the pIIb cell, strong *miR-279* expression is detectable in the late pIIb and pIIIb cells. We conclude that both *miR-279* and Pros are coexpressed during stages of neuronal and sheath cell differentiation.

Pros and *miR-279* define neuron number in MP sensilla

pros and *miR-279* mutants fail to suppress the formation of CO_2 sensory neurons on fly MPs. We next addressed in more detail the development of MP CO_2 neurons in the mutants. To selectively label the neuronal lineage in a mutant sensillum, we used MARCM and Elav-GFP (*elav-GAL4, UAS-mCD8GFP*). In wild-type clones at 45 h APF, Elav-GFP as well as anti-Elav antibody labeled two neurons per single sensillum. Adjacent to each two-neuron cluster, we detected a single Pros-positive cell—the sheath cell (Fig. 5*A*). In contrast, Elav-GFP labeled three neurons in single sensilla in 100% of the analyzed *miR-279* mutants (Fig. 5*B*). In these three neuron sensilla, all neurons expressed Elav. A Pros-positive cell was found closely associated to the cluster (Fig. 5*B*). Mutant MP clones of *pros*^{IG2227} or *pros*^{17}, like *miR-279* clones, displayed three neurons and one sheath cell per sensillum in 100% of *pros*^{IG2227} and 54% of *pros*^{17} mutant palps (Figs. 5*C*,*D*,*G*; 6*D*). Next, we labeled CO_2 neurons with *Gr21-GAL4,UAS-mCD8GFP* in *miR-279* and *pros*^{IG2227} mutant MPs at 70 h APF. A single Gr21a cell positive for Elav was detected per three neuron sensillum in *pros* and *miR-279*

mutant clones (Fig. 5*E*,*F*). In 31% of $pros^{17}$ mutant MPs, Elav-GFP labeled only one single neuron with detectable levels of Elav protein per sensillum (Fig. 6*A*,*B*). In 15.5% of $pros^{17}$ mutant palps, sensilla with up to four cells labeled by Elav-GFP, none of them positive for anti-Elav, were observed, suggesting that these cells are part of the neural lineage but failed to fully differentiate into mature neurons (Fig. 6*C*,*D*). In summary, neuron loss in *pros*-null sensilla shows that in the MP olfactory lineage, Pros helps to establish the neuronal pIIb versus non-neuronal pIIa cell fate (Fig. 6*D*). The hypomorphic alleles of *pros* uncovered an additional role of Pros within the olfactory pIIb lineage. Here, Pros restricts the number of neurons, and thereby prevents the formation of MP CO_2 neurons without affecting number and differentiation of sheath cells (Fig. 6*D*). We conclude that Pros and *miR-279* are required to prevent the formation of an additional neuron, the CO_2 ORN, within Or59c or Or42a ORN-containing MP sensilla of flies.

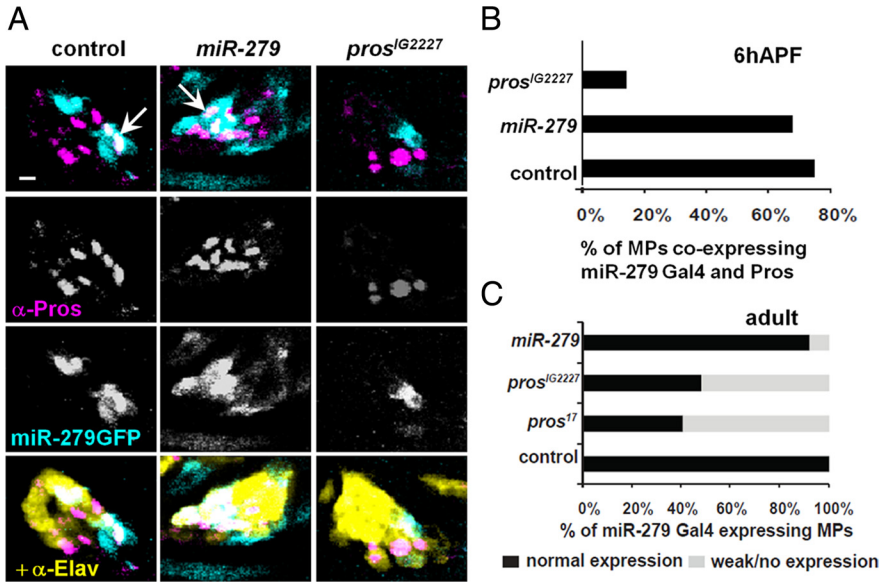

Figure 8. *miR-279* expression is strongly reduced in Pros mutant MPs. ***A***, ***B***, Representative expression patterns of miR-279-GAL4 (turquoise) combined with anti-Pros (pink) and anti-Elav (yellow) staining in control and mutant clones in the developing MP at 6 h APF. Pros and *miR-279* coexpressing cells are indicated with arrows. We detected colabeled cells in 73% ($n = 15$) and 66% ($n = 18$) of control and *miR-279* MPs, respectively. In $pros^{IG2227}$ mutant clones, only 14% ($n = 14$) of the MPs showed cells coexpressing *miR-279* and Pros. ***C***, Expression of *miR-279-GAL4, UAS-mCD8GFP* in adult MPs of wild-type and mutant clones. miR-279-GFP expression is strongly reduced in 59% and 52% of MP of $pros^{17}$ and $pros^{IG2227}$ mutants compared with controls, respectively ($n = 117, 37, 112$). miR-279-GFP expression is only slightly reduced in *miR-279* MP ($n = 107$, 92% compared with controls). Note that efficiency of FLP recombination was not different among the genotypes (data not shown). Scale bars, 5 μm.

miR-279 expression suppresses ectopic MP CO_2 neurons in Pros mutants

We next addressed the functional relationship between *miR-279* and Pros. We inquired whether Pros activity regulates *miR-279* expression during MP olfactory sensilla formation. *miR-279* expression in *miR-279* mutants fully rescued its phenotype (Fig. 7*A*). The same was observed for Pros expression in $pros^{IG2227}$ mutants (Fig. 7*A*). We next expressed *miR-279* in eyFLP clones in the developing MP of $pros^{IG2227}$ mutants. Expression of *miR-279* was sufficient to rescue the phenotype of the hypomorphic allele $pros^{IG2227}$ in 80% of the flies analyzed (Fig. 7*A*). In contrast, expression of Pros in *miR-279*-null mutants suppressed ectopic MP CO_2 neurons in only 37% of the flies analyzed (Fig. 7*A*). Thus, *miR-279* expression in hypomorphic Pros mutants rescues the $pros^{IG2227}$ phenotype to a high degree. We propose that, together with the milder Pros-mediated rescue of *miR-279*-null mutants, Pros acts upstream and also partly in parallel to *miR-279* signaling.

Pros might act as a direct transcriptional activator of *miR-279* expression. In bioinformatics predictions, we detected 18 putative Pros-binding sites in the 2 kb upstream region of *miR-279*, of which we focused on the four most conserved sites. miRs are first transcribed as longer pri-miRs, before they get exported and processed into pre-miR and mature miR by Dicer (Lee et al., 2003). To define the length of the primary *miR-279* transcript, we used 5′RACE, and determined the transcriptional start site at 1.2 kb upstream of the *miR-279* gene (Fig. 7*B*). We used electromobility shift assays (EMSA) to demonstrate direct Pros binding to the *miR-279* enhancer. Purified Pros homeodomain bound strongly only to oligos containing the P4 site as shown by the gel shift (Fig. 7*C*). The shift was significantly reduced when the oligos were mutated to a non-consensus motif. We conclude that Pros protein can bind the *miR-279* upstream putative enhancer regions *in vitro*.

To test whether Pros induces expression of the *miR-279* promoter in a cellular assay, we transfected S2 cells with a *miR-279* promoter construct fused to a firefly luciferase gene (Fig. 7*D* and data not shown). *miR-279* wild-type reporter was strongly expressed in S2 cells, consistent with endogenous *miR-279* expression in these cells (Fig. 7*D*) (Cayirlioglu et al., 2008). To test whether promoter activity was due to endogenous Pros expression in S2 cells, we manipulated Pros levels using RNAi and overexpression. While Pros overexpression did not further increase reporter expression, RNAi against Pros reduced reporter activity by 70 ± 6.2% (Fig. 7*D*). Next, we mutated up to four putative Pros binding-sites in the promoter region (Fig. 7*D*). We observed 42 ± 10% reduced expression of the mutated versus the wild-type

Table 2. Predicted common targets of Pros and *miR-279*

Common target	Gene	Molecular function
CG13906	*nerfin-1*	Transcription factor
CG3758	*escargot*	Transcription factor
CG11988	*neuralized*	Ubiquitin ligase
CG3827	*scute*	Transcription factor
CG9626	*unknown*	Unknown
CG13521	*robo*	Receptor
CG9239	*B4*	Unknown
CG10580	*fringe*	UDP-glycosyltransferase
CG9739	*frizzled-2*	Wnt receptor
CG17835	*invected*	Transcription factor
CG12245	*gcm*	Transcription factor
CG1447	*Ptx1*	Transcription factor
CG6993	*spineless*	Transcription factor
CG1072	*Arrowhead*	Transcription factor
CG18408	*CAP*	Vinculin binding
CG2679	*goliath*	Transcription factor
CG9623	*inflated*	Receptor cell adhesion
CG1004	*rhomboid*	Serine-type peptidase, cleaves EGF
CG5507	*Transcript 48*	Unknown
CG31048	*unknown*	Unknown

List of the twenty predicted target genes shared between Pros and *miR-279*. Genes include transcription factors and enzymes implicated in neuronal development.

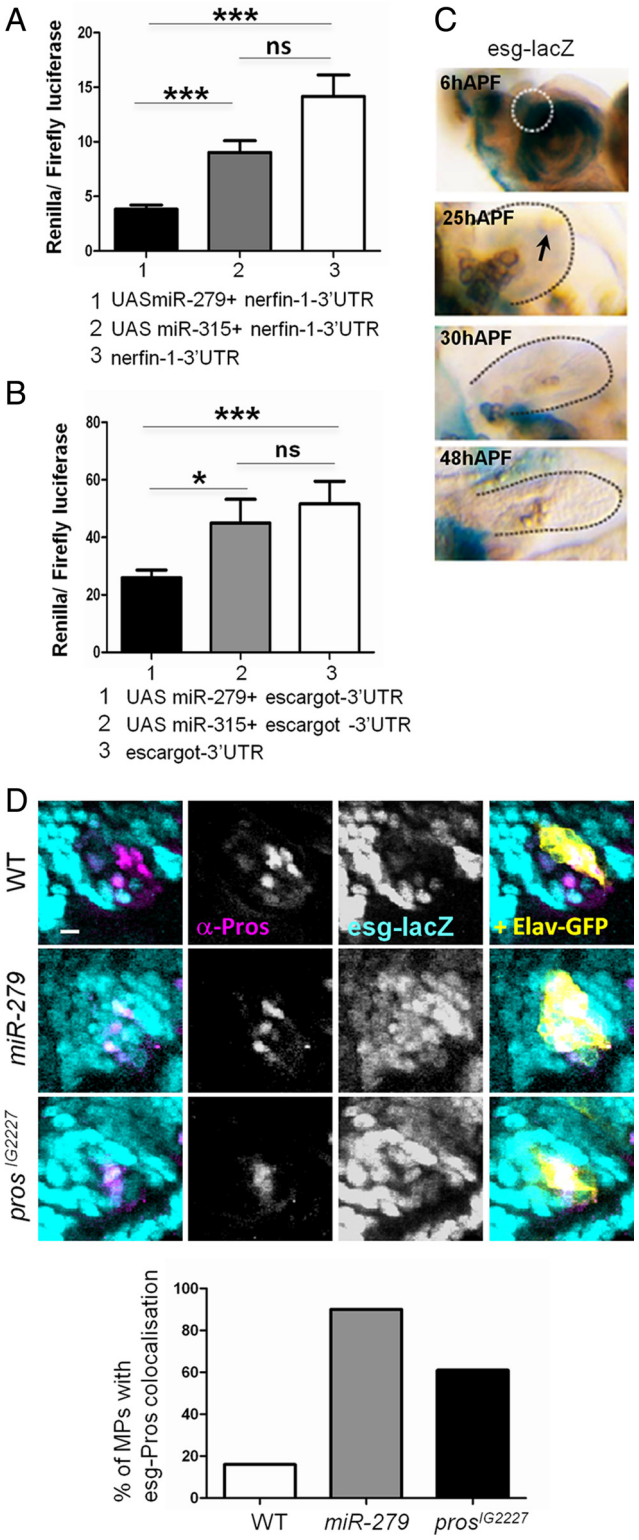

Figure 9. Escargot and Nerfin-1 are shared target of *miR-279* and Prospero. ***A***, Quantification of S2 cell assays using nerfin-3′UTR reporter with and without overexpression of *miR-279* or *miR-315*. Experiments were performed in triplicates and data from four repetitions are pooled. ***B***, Quantification of S2 cell assays with esg 3′UTR and overexpression of *miR-279* or *miR-315*. Overexpression of *miR-279* reduced esg-3′UTR reporter expression to 51 ± 9%. ***C***, MPs of different developmental stages: LacZ (blue) staining and anti-βGal (turquoise) immunoreactivity reflects expression of esg (*P[lacZ]esg*). At 6 h APF, esg-lacZ is seen strongly in cells of the antennal disc, including the future MP (circled area). At 25 h APF, esg-lacZ is expressed at much lower levels in the MP. No expression was detected in MPs at 30 or 48 h APF (arrow). ***D***, MPs at 6 h APF from control and mutant flies carrying an esg-lacZ. Esg expression was visualized using anti-βGal (esg-lacZ), expression of Elav was monitored with anti-GFP, and Pros was labeled with anti-Pros. Coexpression of Pros with esg was analyzed in the area of control or mutant clone (Elav-GFP, yellow). In the control case, only 16% of MPs have double-labeled cells ($n = 12$). In the absence of *miR-279* or Pros, repression of esg expression in the developing MP is released. In *miR-279* and *pros*^{IG2227} mutants, 90% ($n = 11$) and 61% ($n = 13$) of the MPs, respectively, counted show cells with Pros-esg coexpression. Scale bars, 5 μm.

promoter construct (Fig. 7*D*). We tested the effect of Pros RNAi and Pros overexpression on the mutated promoter. Similar to the wild-type construct, Pros overexpression did not significantly increase enhancer activity, while Pros RNAi reduced activity levels to 49 ± 7%, similar to the wild-type reporter (Fig. 7*D*). These data suggest that Pros is required for expression of *miR-279* in S2 cells. Nevertheless, they also indicate that additional sites of the 18 predicted Pros binding-sites might be involved.

To test the binding of Pros to the *miR-279* promoter *in vivo*, we performed ChIP. We analyzed chromatin from embryos that overexpress FLAG-tagged Pros, and immunoprecipitated Pros-FLAG with α-FLAG antibody. PCR was used to amplify the region flanking the P4 binding site. Forty-eight percent of the input DNA was immunoprecipitated using α-FLAG, whereas control IgG and α-FLAG without input did not produce a detectable PCR product (Fig. 7*E*). The resulting PCR product was sequenced to confirm that it contained P4 Pros binding site in the promoter of *miR-279* (Fig. 7*E*).

We then investigated the effect of loss of Pros on the expression of *miR-279 in vivo*. To this aim, we used the *miR-279-GAL4* driver line, described above, to monitor *miR-279* expression in control, *miR-279*, and *pros* mutant MP clones during development and adulthood. At 6 h APF, *miR-279* expression is first detected in Pros-positive cells in the developing MP. At this time point, *miR-279* expression in Pros-expressing cells was detected in only 16% of the *pros*^{IG2227} MPs compared with in 75% of the wild-type and 69% of the *miR-279* mutant MPs (Fig. 8*A*,*B*). Similar results were obtained in adult MPs (Fig. 8*C*). The reduction in *miR-279* expression in *pros* mutants correlated well with the proportion of *pros*^{IG2227} MPs that showed a high number of MP CO_2 neurons (43%: >15; 54%: >12; 70%: >10 CO_2 neurons; compare Fig. 1). These data show that Pros activity contributes to the expression of *miR-279* in MPs.

We conclude that Pros directly binds the *miR-279* enhancer and contributes to its expression to suppress the formation of ectopic CO_2 neurons in the fly MP.

Common targets Escargot and Nerfin-1 are sufficient to induce MP CO_2 neurons

Previously, *in vivo* Pros/DNA-interaction sites were mapped in the fly embryo (Choksi et al., 2006). Identification of putative miR targets has been quite successful using several bioinformatic analysis tools. We combined the predicted *miR-279* targets from three different databases and compared them to the list of *in vivo* Pros targets. Twenty Pros target genes were predicted to be *miR-279* targets (Table 2). Next, we used GO analysis to assess the putative role of the common targets of Pros and *miR-279*. Shared targets fell into six categories, with 12 of 20 targets falling into two GO terms—cell fate determination and nervous system development (data not shown). Thus, they appeared highly relevant for the described phenotype and were the focus of our further analysis. These predictions suggested that *miR-279* might act on Pros target genes, being a Pros-target itself.

Two high-ranking *miR-279* targets and *in vivo* targets of Pros are the snail-family transcription factor Escargot (Esg) and the

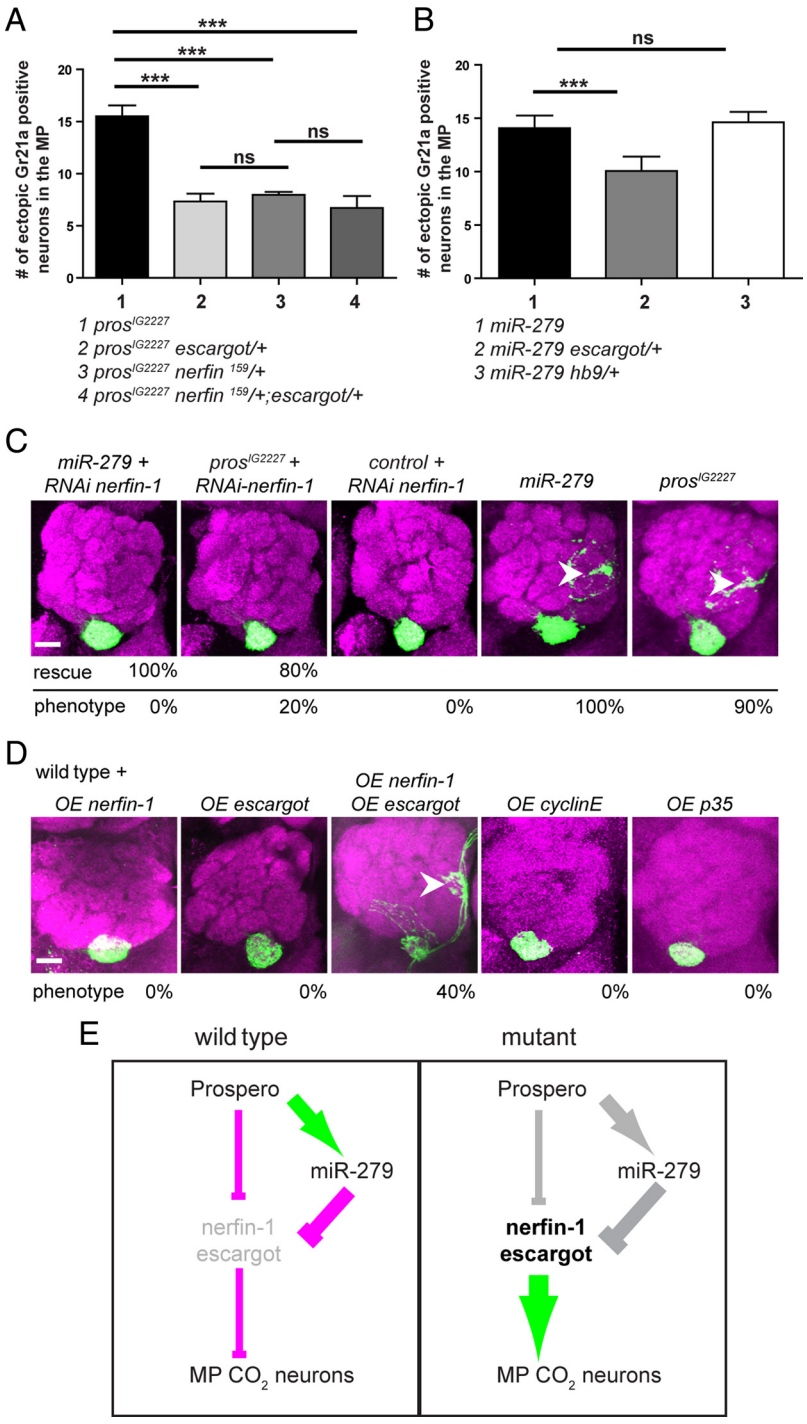

Figure 10. Increased expression of Nerfin-1 and Escargot is required and sufficient to induce CO_2 neuron formation and mistargeting on the MP. ***A***, Genetic interaction of $pros^{IG2227}$ and two target genes *nerfin-1* and *esg*. The number of ectopic Gr21a-positive cells in $pros^{IG2227}$ mutant MPs missing either one allele of *esg*, *nerfin-1*, or both *esg* and *nerfin-1* is reduced by 55% ($n = 22$), 49% ($n = 30$), and 40% ($n = 20$) compared with controls ($n = 37$), respectively. ***B***, Quantification of the genetic interaction of *miR-279* and *esg* showing a reduction by 44% of the ectopic Gr21a neurons after removal of one copy of *esg* in the *miR-279* mutant background ($n = 30$) compared with *miR-279* mutant only ($n = 30$). The removal of one copy *hb9* (*exex*) did not result in a reduced number of ectopic CO_2 neurons ($n = 24$). ***C***, *nerfin-1-RNAi* expression in the background of the *miR-279* and the $pros^{IG2227}$ background rescues the phenotype by 100% ($n = 35$) and 80% ($n = 29$), respectively. *Nerfin-1 RNAi* in control flies induced no phenotype ($n = 20$). ***D***, Overexpression of targets in the wild-type background. Single overexpression of Nerfin-1 and Esg did not result in Gr21a medial mistargeting. In contrast, overexpression of both Esg plus Nerfin-1 phenocopied the phenotype of *miR-279* and $pros^{IG2227}$ in 40% ($n = 24$) of all fly brains analyzed. Overexpression of the apoptosis inhibitor p35 ($n = 20$) and the cell cycle gene CyclinE ($n = 25$) did not result in a *miR-279*-like phenotype. ***E***, Mechanistic model of a network of Pros, *miR-279*, Nerfin-1, and Escargot: In wild-type MPs, Pros directly binds and represses the expression of at least two target genes, *nerfin-1* and *escargot*. In a parallel pathway, Pros directly activates the expression of *miR-279*, which in turn represses *nerfin-1* and *esg* on a posttranscriptional level. Our genetic data indicate that indirect repression via *miR-279* post-transcriptionally is more powerful compared with direct Pros repression on the genomic level (indicated by line thickness). This regulation represses the formation of MP CO_2 neurons. In *pros* or *miR-279* mutants, the repression of Nerfin-1 and Esg expression directly and/or indirectly is lost. As a consequence, an excess of Nerfin-1 and Esg leads to the formation of ectopic CO_2 neurons within Or42a and Or59c olfactory sensilla on the MP. Scale bars, 20 μm.

neurogenic zinc-finger transcription factor Nerfin-1 (Kuzin et al., 2005; Choksi et al., 2006). We used a *P*[*lacZ*] insertion into the *esg* locus to analyze Esg expression *in vivo*. While at 6 h APF, Esg was expressed in the developing MP and was low or excluded from Pros-expressing pIIb cells. At later stages (25, 30, and 48 h APF), Esg expression appeared overall lower and went down to finally undetectable levels (Fig. 9*C*). Similar to Esg, Nerfin-1 is also expressed in the developing MP at low levels (Cayirlioglu et al., 2008). Therefore, Esg is expressed at the right time and place to act as a downstream target of Pros and *miR-279* during MP olfactory sensilla development.

To test whether *miR-279* can silence the expression of Esg via the 3′UTR *in vitro*, we assayed 3′UTR-luciferase reporter activity in S2 cells. These reporter constructs carried the coding region of the renilla luciferase followed by the 3′UTR of the respective target gene. *miR-279* overexpression significantly silenced the expression of the esg 3′UTR and the nerfin-1 3′UTR reporter constructs (Fig. 9*A*,*B*). The expression of the esg 3′UTR and the nerfin-1 3′UTR were reduced to 51 ± 9% and to 27 ± 10%, respectively (Fig. 9*A*,*B*). Therefore, Esg and Nerfin-1 are direct targets of *miR-279 in vitro*.

To test the impact of *miR-279* and $pros^{IG2227}$ on Esg expression *in vivo*, we crossed the esg-P[lacZ] into the mutant background of *miR-279* and $pros^{IG2227}$ (Fig. 9*D*). We analyzed MPs at 6 h APF. In control palps, a low percentage (16%) of MPs displayed coexpression of Pros and β-gal (esg), while in *miR-279* and $pros^{IG2227}$ mutant clones, the colocalization of Pros and esg[lacZ] occurred in up to 90% and 61% of all palps analyzed, respectively. We conclude that *miR-279* as well as Pros can repress the expression of Esg *in vitro* and *in vivo*.

We showed previously that reduction of Nerfin-1 expression by removing one allele of *nerfin-1* in the background of *miR-279* mutants ameliorated the ectopic CO_2 neuron phenotype (Cayirlioglu et al., 2008). Using the same experimental set-up for $pros^{IG2227}$ mutants, we found that reduction of Nerfin-1 reduced the

number of ectopic CO_2 neurons significantly by 55% compared with $pros^{IG2227}$ mutant palps only (Fig. 10*A*). In MPs of *miR-279* and $pros^{IG2227}$ flies, reduction of *esg* reduced the number of ectopic CO_2 neurons by 29% and 49%, respectively (Fig. 10*A*,*B*). Removal of one copy of both *nerfin-1* and *esg* in the background of $pros^{IG2227}$ did not further reduce the number of ectopic CO_2 neurons (Fig. 10*A*). Hb9 (exex), a predicted target of *miR-279*, but not a target of Pros, did not show a genetic interaction with *miR-279* (Fig. 10*B*). We conclude that shared *miR-279* and Pros target genes are required for CO_2 neuron formation on MPs.

To address the role of Nerfin-1 during axon targeting, we expressed an RNAi construct against *nerfin-1* in *miR-279*, *pros*, and control palps. *Nerfin-1* RNAi was able to rescue the *miR-279*- and $pros^{IG2227}$-targeting phenotype in 100% and 80% of all flies analyzed, respectively, but had no effect on CO_2 neurons in wild-type clones (Fig. 10*C*). A similar experiment with *esg* was not possible in lieu of a working RNAi construct. We tested four additional potential downstream factors of *miR-279* and Pros for interaction with *pros* or *miR-279* mutants by means of *in vivo* RNAi: *spineless*, *senseless*, *gcm*, and *Ptx-1*. None of them rescued the targeting defect of *miR-279* or *pros* mutants (data not shown).

To test whether elevated levels of Nerfin-1 and Esg are sufficient to induce the formation and mistargeting of CO_2 neurons, we overexpressed Esg and Nerfin-1 separately or together in wild-type MP clones. Overexpression of only Nerfin-1 or Esg did not result in an altered targeting pattern of CO_2 neurons (Fig. 10*D*). In contrast, overexpression of both targets together phenocopied the *miR-279* and *pros* phenotype in 40% of all flies analyzed (Fig. 10*D*). Overexpression of *p35* and *cyclinE* in the wild-type background did not induce ectopic CO_2 neurons and mistargeting, suggesting that lack of apoptosis or altered cell cycle progression are not sufficient to induce ectopic CO_2 neurons (Fig. 10*D*).

These experiments led us to propose a genetic network including the activities of Pros, *miR-279*, and two shared downstream target genes. We provide evidence that Pros is a positive regulator of *miR-279* expression. *miR-279* in turn represses at least two of Prospero's targets. Upregulation of Esg and Nerfin-1 is sufficient for the formation and mistargeting of MP CO_2 neurons. In conclusion, we suggest that Pros uses its transcriptional activator activity to enhance its own repressor function via the induction and activity of a single microRNA, *miR-279* (Fig. 10*E*).

Discussion

Here, we show that the transcription factor Pros prevents the formation of MP CO_2 neurons by inducing *miR-279* to enhance its own repressor activity on two shared target genes, *nerfin-1* and *esg* (Fig. 10). We first describe the expression of Pros and *miR-279* during the formation of two neurons in the MP wild-type neural lineage. Second, we demonstrate that Pros and *miR-279* are required to prevent the formation of a third ORN within certain MP sensilla. Third, we present evidence that Pros regulates *miR-279* expression *in vivo*, possibly by direct binding to the *miR-279* enhancer. Fourth, we show that re-expression of *miR-279* in *pros* mutant clones rescues the *pros* phenotype. Finally, we find that increased levels of two Pros and *miR-279* target genes, Nerfin-1 and Escargot, induces the formation and mistargeting of MP CO_2 neurons. We propose a genetic network in which Pros uses two activity modes—one direct and one indirect via *miR-279* activation—to repress target genes *Nerfin-1* and *Esg* (Fig. 10). This fine-tuning of Pros activity defines the number of neurons in two specific olfactory sensilla and thereby prevents the expression of a CO_2 neuron genetic program on MPs.

Pros together with *miR-279* defines neuron numbers in specific olfactory sensilla

Our analysis of both wild-type and mutant olfactory lineages suggests that the development of MP olfactory sensilla follows the canonical lineage model (Lai and Orgogozo, 2004). Previous analysis of the role of Pros in ES and antennal olfactory sensilla suggested that complete loss of Pros results in an early phenotype in the sensory organ lineage. It affects the proper establishment of the pIIb cell that ultimately gives rise to all neurons and the sheath cell in each sensillum (Manning and Doe, 1999; Reddy and Rodrigues, 1999; Sen et al., 2003). In agreement with this work, we also find that *pros*-null mutants showed neuron loss in several classes of ORNs, including antennal CO_2 neurons. Interestingly, we describe a new hypomorphic allele of *pros* and reveal that Pros also has a later role during the definition of neuron number in specific olfactory sensilla. This function of Pros is similar to its described role in the embryonic CNS, where Pros presumably uses its repressor activity to prevent mitosis (Choksi et al., 2006). *miR-279*-null mutants, in contrast to *pros*-null mutants, do not display neuron loss but, like *pros* hypomorphic mutants, fail to repress the formation of an extra CO_2 neuron in two classes of MP sensilla. Thus, *miR-279* is selectively required during the second Pros phase uncovered in the *pros* hypomorphic alleles. Using this mechanism, *miR-279*-mediated repression downstream of Pros appears to impose functional specificity on this pleiotropic neural development regulator.

Despite the expression of Pros and *miR-279* in all olfactory sensilla, Pros' and *miR-279*'s function in CO_2 neuron repression appears restricted to the MP. Although we currently cannot answer why Pros and *miR-279* affect MP sensilla differently than antennal sensilla, we speculate that the reason might be linked to the different developmental and evolutionary origin of these organs that depend on two different proneural genes, *Atonal* and *Amos* (Jhaveri et al., 2000; Markitantova et al., 2003). Similar to the three ORN mutant MP sensillum in the fly, the wild-type CO_2 sensory neuron of mosquito also belongs to the Ato lineage and resides in a three-neuron sensillum on the MP (Lu et al., 2007).

It is possible that some olfactory sensilla are especially sensitive to Pros signaling. Work in the ES lineage has shown that Notch and Pros can cooperate to prevent additional mitosis of pIIIb cells in the lineage (Simon et al., 2009). Notch is also involved in regulation of neuron type and targeting in the olfactory system (Endo et al., 2007). Given the variety of olfactory bristles with different neuron numbers and types, differential sensitivity to levels of lineage determinants such as Pros, possibly due to different Notch activities, could have contributed to the formation of subsets of this large repertoire.

microRNAs and Prospero in cell fate decisions

miRs have been implicated in stabilizing gene expression by engaging in different modes of feedback regulation (Herranz and Cohen, 2010). They are posttranscriptional repressors of gene expression, which makes them perfectly suited for fine-tuning or tightly controlling expression levels of genes (Biryukova et al., 2009; Coolen and Bally-Cuif, 2009; Liu et al., 2009). Here, we provide evidence that Pros regulates *miR-279* activity to suppress its own target genes. Why does Prospero engage a microRNA? We envision three scenarios: (1) Pros repressor activity on the genomic level is simply too weak, (2) Pros acting on the transcriptional level is not fast enough, and (3) Pros uses *miR-279* not only to enhance and speed up its activity but also to temporally define expression levels. The observation that re-expression of Pros in *miR-279* mutants rescued the *miR-279* phenotype to a certain

degree is consistent with a role of *miR-279* as enhancer of repressor activity. *miR-279* mutants phenocopy only a specific aspect of the *pros* phenotype. This argues for a role of *miR-279* in temporal control of Pros activity.

We showed that overexpression of two shared targets of Pros and *miR-279* Nerfin-1 together with Esg was sufficient to induce MP CO_2 neurons. Nerfin-1 and Esg reduction lowers the numbers of ectopic CO_2 neurons in *miR-279* and *pros* mutants. Thus, Nerfin-1 and Esg are essential and sufficient to trigger CO_2 neuron formation in MP, suggesting that they are part of a MP CO_2 neuron program normally suppressed in flies. Consistent with a role as possible axon targeting factor, Nerfin-1 was shown previously to be essential for axon guidance decisions in the developing embryonic CNS. *nerfin-1* mutants failed to properly express guidance factors such as robo2, wnt5, derailed, G-oalpha47A, Lar, and futsch (Kuzin et al., 2005). Our data, together with previous analysis of *esg* mutants (Yang et al., 2010), points to a role in neurogenesis. However, single mutants of *esg* did not show a defect in antennal CO_2 neuron development (data not shown). Simple interference with cell cycle progression or apoptosis was not sufficient to induce ectopic CO_2 neurons, arguing for a more complex biology controlled by both Nerfin-1 and Esg. Future analysis will address the relationship and exact function of Nerfin-1 and Esg.

Divergence of CO_2 sensory systems of fruit flies and mosquitoes

MP ORN axons in fruit flies and mosquitoes target medial glomeruli in the AL. This is also the case for the axons of the ectopic CO_2 neurons in the mutant fly MP. It is possible that certain developmental constraints on the wiring of the olfactory neurons to the AL make it difficult for MP neurons not to innervate food-related glomeruli in the AL (Ghysen, 1992; Sweeney et al., 2007). Thus, it might have been more feasible to relocate the neurons and take advantage of an existing wiring program than to leave the neurons in the same sensillum and redirect them to a new glomerulus. The pathway we describe here might have contributed to the differential localization of CO_2 neurons in insects with opposite CO_2 preferences. *pros*, *miR-279*, as well as *nerfin-1* and *escargot* genes are present in the mosquito genome. We speculate that the genetic and functional interaction of Pros, *miR-279*, Nerfin-1, Escargot, and likely additional factors was either lost in mosquito or acquired in the fly to allow or prevent the formation of MP CO_2 neurons, respectively. In support of this, we analyzed putative target genes for *Anopheles gambiae miR-279* (*aga-miR-279*) using miRBase prediction. Notably, both *aga-escargot* and *aga-nerfin-1* are not among the first 150 predicted targets of *aga-miR-279* (see Materials and Methods, above). Given that overexpression of Nerfin-1 and Esg are sufficient to induce MP CO_2 neurons, it is possible that Nerfin-1 and Esg are key factors in a CO_2 neuron program actively suppressed by both Pros and *miR-279* in fly MPs. Hence, although the relocation of CO_2 neurons from antenna to MP might be a rather unusual or extreme case, it is conceivable that this pathway or similar miR-mediated mechanisms could have been used to produce sensilla, including nonolfactory sensilla, of different neuronal numbers in different species.

Is MP location and medial mistargeting sufficient to convert repulsion into attraction? MP CO_2 neurons in the mutants are functional. Mutant flies with antennae still avoid CO_2, while antennaless mutants appear indifferent to CO_2 (data not shown). One of many interpretations of these data is that MP CO_2 ORNs activate attraction and repulsion glomeruli simultaneously, resulting in behavioral indifference. Nevertheless, it has been reported that individual glomeruli mediate innate attraction versus repulsion (Semmelhack and Wang, 2009).

In conclusion, our study identifies the first miR regulated by transcriptional activity of Pros that represses Pros target molecules. We propose that miR-mediated regulation of pleiotropic neural genes played a role in the divergence of sensory systems. Failure of miR-mediated fine-tuning of intrinsically noisy genetic pathways could have created opportunities for nervous system divergence. Thus, this mode of activity restriction presents an attractive alternative to enhancer-mediated divergence of protein expression during evolution.

References

Beissbarth T, Speed TP (2004) GOstat: find statistically overrepresented gene ontologies within a group of genes. Bioinformatics 20:1464–1465.

Biryukova I, Asmar J, Abdesselem H, Heitzler P (2009) *Drosophila* mir-9a regulates wing development via fine-tuning expression of the LIM only factor, dLMO. Dev Biol 327:487–496.

Cayirlioglu P, Kadow IG, Zhan X, Okamura K, Suh GS, Gunning D, Lai EC, Zipursky SL (2008) Hybrid neurons in a microRNA mutant are putative evolutionary intermediates in insect CO2 sensory systems. Science 319:1256–1260.

Choksi SP, Southall TD, Bossing T, Edoff K, de Wit E, Fischer BE, van Steensel B, Micklem G, Brand AH (2006) Prospero acts as a binary switch between self-renewal and differentiation in *Drosophila* neural stem cells. Dev Cell 11:775–789.

Cook T, Pichaud F, Sonneville R, Papatsenko D, Desplan C (2003) Distinction between color photoreceptor cell fates is controlled by Prospero in *Drosophila*. Dev Cell 4:853–864.

Coolen M, Bally-Cuif L (2009) MicroRNAs in brain development and physiology. Curr Opin Neurobiol 19:461–470.

de Bruyne M, Clyne PJ, Carlson JR (1999) Odor coding in a model olfactory organ: the *Drosophila* maxillary palp. J Neurosci 19:4520–4532.

Endo K, Aoki T, Yoda Y, Kimura K, Hama C (2007) Notch signal organizes the *Drosophila* olfactory circuitry by diversifying the sensory neuronal lineages. Nat Neurosci 10:153–160.

Ghysen A (1992) The developmental biology of neural connectivity. Int J Dev Biol 36:47–58.

Gibson G (1996) Genetics, ecology and behaviour of anophelines. Ciba Found Symp 200:22–37; discussion 37–47.

Grant AJ, Wigton BE, Aghajanian JG, O'Connell RJ (1995) Electrophysiological responses of receptor neurons in mosquito maxillary palp sensilla to carbon dioxide. J Comp Physiol A 177:389–396.

Grosjean Y, Balakireva M, Dartevelle L, Ferveur JF (2001) PGal4 excision reveals the pleiotropic effects of Voila, a *Drosophila* locus that affects development and courtship behaviour. Genet Res 77:239–250.

Herranz H, Cohen SM (2010) MicroRNAs and gene regulatory networks: managing the impact of noise in biological systems. Genes Dev 24:1339–1344.

Jhaveri D, Sen A, Reddy GV, Rodrigues V (2000) Sense organ identity in the *Drosophila* antenna is specified by the expression of the proneural gene atonal. Mech Dev 99:101–111.

Jones WD (2008) MicroRNA mutant turns back the evolutionary clock for fly olfaction. Bioessays 30:621–623.

Jones WD, Cayirlioglu P, Kadow IG, Vosshall LB (2007) Two chemosensory receptors together mediate carbon dioxide detection in *Drosophila*. Nature 445:86–90.

Kuzin A, Brody T, Moore AW, Odenwald WF (2005) Nerfin-1 is required for early axon guidance decisions in the developing *Drosophila* CNS. Dev Biol 277:347–365.

Kwon JY, Dahanukar A, Weiss LA, Carlson JR (2007) The molecular basis of CO2 reception in *Drosophila*. Proc Natl Acad Sci U S A 104:3574–3578.

Lai EC, Orgogozo V (2004) A hidden program in *Drosophila* peripheral neurogenesis revealed: fundamental principles underlying sensory organ diversity. Dev Biol 269:1–17.

Lebreton G, Faucher C, Cribbs DL, Benassayag C (2008) Timing of Wingless signalling distinguishes maxillary and antennal identities in *Drosophila* melanogaster. Development 135:2301–2309.

Lee Y, Ahn C, Han J, Choi H, Kim J, Yim J, Lee J, Provost P, Rådmark O, Kim

S, Kim VN (2003) The nuclear RNase III Drosha initiates microRNA processing. Nature 425:415–419.

Liu SP, Fu RH, Yu HH, Li KW, Tsai CH, Shyu WC, Lin SZ (2009) MicroRNAs regulation modulated self-renewal and lineage differentiation of stem cells. Cell Transplant 18:1039–1045.

Lu T, Qiu YT, Wang G, Kwon JY, Rutzler M, Kwon HW, Pitts RJ, van Loon JJ, Takken W, Carlson JR, Zwiebel LJ (2007) Odor coding in the maxillary palp of the malaria vector mosquito Anopheles gambiae. Curr Biol 17:1533–1544.

Manning L, Doe CQ (1999) Prospero distinguishes sibling cell fate without asymmetric localization in the *Drosophila* adult external sense organ lineage. Development 126:2063–2071.

Markitantova YV, Makariev EO, Pavlova GV, Zinovieva RD, Mitashov VI (2003) Location of the Prox1 gene expression during newt lens and retina regeneration. Dokl Biol Sci 391:361–364.

Ramdya P, Benton R (2010) Evolving olfactory systems on the fly. Trends Genet 26:307–316.

Reddy GV, Rodrigues V (1999) Sibling cell fate in the *Drosophila* adult external sense organ lineage is specified by prospero function, which is regulated by Numb and Notch. Development 126:2083–2092.

Sandmann T, Jensen LJ, Jakobsen JS, Karzynski MM, Eichenlaub MP, Bork P, Furlong EE (2006) A temporal map of transcription factor activity: mef2 directly regulates target genes at all stages of muscle development. Dev Cell 10:797–807.

Semmelhack JL, Wang JW (2009) Select *Drosophila* glomeruli mediate innate olfactory attraction and aversion. Nature 459:218–223.

Sen A, Reddy GV, Rodrigues V (2003) Combinatorial expression of Prospero, Seven-up, and Elav identifies progenitor cell types during sense-organ differentiation in the *Drosophila* antenna. Dev Biol 254:79–92.

Simon F, Fichelson P, Gho M, Audibert A (2009) Notch and Prospero repress proliferation following cyclin E overexpression in the *Drosophila* bristle lineage. PLoS Genet 5:e1000594.

Suh GS, Wong AM, Hergarden AC, Wang JW, Simon AF, Benzer S, Axel R, Anderson DJ (2004) A single population of olfactory sensory neurons mediates an innate avoidance behaviour in *Drosophila*. Nature 431:854–859.

Sweeney LB, Couto A, Chou YH, Berdnik D, Dickson BJ, Luo L, Komiyama T (2007) Temporal target restriction of olfactory receptor neurons by Semaphorin-1a/PlexinA-mediated axon-axon interactions. Neuron 53:185–200.

Vosshall LB, Stocker RF (2007) Molecular architecture of smell and taste in *Drosophila*. Annu Rev Neurosci 30:505–533.

Yang DJ, Chung YJ, Lee SJ, Park SY, Pyo JH, Ha NC, Yoo MA, Park BJ, (2010) Slug, mammalian homologue gene of *Drosophila* escargot promotes neuronal differentiation through suppression of HEB/daughterless. Cell Cycle 9:2789–2802.